

REVIEW • OPEN ACCESS

The Coordinated Universal Time (UTC)

To cite this article: G Panfilo and F Arias 2019 *Metrologia* **56** 042001

View the [article online](#) for updates and enhancements.

You may also like

- [UTC\(OP\) based on LNE-SYRTE atomic fountain primary frequency standards](#)
G D Rovera, S Bize, B Chupin et al.
- [A first step towards the introduction of redundant time links for the generation of UTC: the calculation of the uncertainties of \[UTC-UTC\(k\)\]](#)
G Panfilo, G Petit and A Harmegnies
- [Achieving traceability to UTC through GNSS measurements](#)
P Defraigne, J Achkar, M J Coleman et al.

Review

The Coordinated Universal Time (UTC)

G Panfilo¹ and F Arias^{2,3}¹ International Bureau of Weights and Measures (BIPM), Pavillon de Breteuil 92312 Sèvres, France² SYRTE, Observatoire de Paris, Université PSL, CNRS, Sorbonne Université, LNE, 61 avenue de l'Observatoire 75014, Paris, FranceE-mail: gpanfilo@bipm.org

Received 11 December 2018, revised 19 March 2019

Accepted for publication 1 May 2019

Published 18 June 2019

**Abstract**

Coordinated Universal Time (UTC) has considerably changed in recent years. The evolution of UTC follows the scientific and industrial progress by developing appropriate models, more adapted calculation algorithms, more efficient and rapid dissemination processes and a well defined traceability chain. The enormous technical progress worldwide has resulted in an impressive number of atomic clocks now available for UTC calculation. The refined time and frequency transfer techniques are approaching the accuracy requested for the new definition of the SI second. The more regular operation of primary frequency standards (PFS) increases the accuracy of UTC and opens a possible new development for time scale algorithms. From the metrological point of view all the ingredients are available for major improvements to UTC. Dissemination of UTC is done by the monthly publication of results in BIPM *Circular T*. This document makes a quality evaluation of local representations of UTC, named UTC(*k*), in national institutes, and other organizations, by giving the evolution of their offsets relative to UTC and their respective uncertainties. The clock models adopted and the time transfer techniques have progressively improved over the years, assuring the long-term stability of UTC. Each computation of UTC processes data over one month with five-day sampling and publication. A rapid solution of UTC (UTC_r) has existed since 2013, and consists of the processing of daily sampled data over four consecutive weeks, computed and published weekly. It gives quick access to UTC, and allows participating laboratories to better monitor the offsets of their realizations to the reference UTC. The traditional monthly publication, containing results of all the laboratories contributing data to the BIPM for the computation of UTC was complemented after the establishment of the Mutual Recognition Arrangement of the International Committee on Weights and Measures (CIPM MRA). This time comparison, which has been the responsibility of the BIPM since 1988, added as a complement the key comparison on time defined by the Consultative Committee for Time and Frequency (CCTF) in 2006 as CCTF-K001.UTC, where the results published are those of national metrology institutes (NMIs) signatories of the CIPM MRA, or designated institutes (DIs). The traceability issues are formalized in the framework of the CIPM MRA. The development of time metrology activities in the different metrology regions, supports the actions of the BIPM time department to improve the accuracy of [UTC–UTC(*k*)], where the coordination with the Regional Metrology Organizations (RMOs) has a key role. This paper presents an overview of UTC.

Keywords: UTC, time transfer, algorithms, primary frequency standard

(Some figures may appear in colour only in the online journal)

³ Retired from BIPM on 30 November 2017.

List of used acronyms

AFRIMETS	Intra-Africa Metrology System	ITU	International Telecommunication Union
AOS	Astrodynamical Observatory, Space Research Centre P.A.S. (Poland)	ITU-R	Radiocommunication Sector of the International Telecommunication Union
AV	All in view	IGS	International GNSS Service
APMP	Asia Pacific Metrology Programme	IGST	Timescale of the IGS
BeiDou	Chinese Global navigation satellite system	IT/INRIM	Istituto Nazionale di Ricerca Metrologica (Italy)
BIH	Bureau international de l'heure	ITU-R TF	International Telecommunication Union Radiocommunication Sector, Time signals and frequency standards emissions Series
BIPM	International Bureau of Weights and Measures—Bureau international des poids et mesures	KC	Key comparison
CCDS	Consultative Committee for the Definition of the Second	KCDB	Key comparison database
CCTF	Consultative Committee for Time and Frequency	KRISS/KRIS	Korea Research Institute of Standards and Science (Rep. of Korea)
CGGTTS	special format and procedure for GPS data tracking and averaging	MJD	Modified julian date
CGPM	General Conference on Weights and Measures	NICT	National Institute of Information and Communications Technology (Japan)
CH/METAS	Conférence générale des poids et mesures	NIM	National Institute of Metrology (P.R. China)
CIPM	Federal Institute of Metrology (Switzerland)	NMI	National Metrological Institute
	International Committee for Weights and Measures—Comité international des poids et mesures	NPL	National Physical Laboratory (United Kingdom)
CLS	Collecte Localisation Satellites	NTSC	National Time Service Center of China (P.R. China)
CNES	Centre national d'études spatiales	NIST	National Institute of Standards and Technology (USA)
COOMET	Euro-Asian Cooperation of National Metrological Institutions	OP/LNE-SYRTE	Laboratoire national de métrologie et de mesures, Systèmes de référence Temps-Espace, Observatoire de Paris (France)
CV	common-view	PFS	Primary Frequency Standard
EAL	Free atomic time scale, échelle atomique libre	PL	Consortium of laboratories in Poland
EURAMET	European Association of National Metrology Institutes	PTB	Physikalisch-Technische Bundesanstalt (Germany)
GAGAN	GPS Aided GEO Augmented Navigation Galileo	QZSS	Japanese Regional navigation satellite system
GLONASS	Europe Global navigation satellite system	RISE/SP	Sveriges Provnings- och Forskningsinstitut (Swedish National Testing and Research Institute) (Sweden)
GNSS	Russian Global Navigation Satellite System	RINEX	Receiver Independent Exchange Format
GPS	Global Navigation Satellite System	ROA	Real Instituto y Observatorio de la Armada (Spain)
GPS PPP	US Global Positioning System	RMO	Regional metrology organization
	or PPP for short: GPS carrier-phase Precise Point Positioning solution for time and frequency transfer	SATRE	TWSTFT, SATRE link or SATRE for short: TWSTFT using the SATellite Time and Ranging Equipment (hardware emitting-receiving modem)
GPS IPPP	or IPPP for short: GPS carrier-phase with integer ambiguity resolution for time and frequency transfer	SI	International System of Units
GPS P3	The GPS links obtained using dual-frequency receivers	SDR TWSTFT	SDR link or SDR for short: TWSTFT with data from Software-Defined Radio receivers
GPS MC	GPS Multi Channel	SFS	Secondary Frequency Standard, formally Secondary Representation of the Second (SRS)
GPS SC	GPS Single Channel	SIM	Inter-American Metrology System
GPSGLN	GPS and GLONASS time link combination technique	SU/VNIIFTRI	Russian Institute of Metrology for Time and Space
GULFMET	Gulf Association for Metrology		
GUM	Central Office of Measures (Poland)		
IAG	International Association of Geodesy		
IAU	International Astronomical Union		
IERS	International Earth Rotation and Reference Systems Service		
IRNSS	Indian Regional navigation satellite system		

TAI	International Atomic Time
TL	Telecommunications Laboratory (Chinese Taipei)
TT	Terrestrial Time
TWGPPP	Combined time link technique GPS PPP and TWSTFT
TWSTFT, or TW for short	Two Way Satellite Time and Frequency Transfer
URSI	International Union of Radio Sciences
USNO	U.S. Naval Observatory (USA)
UT1	Universal Time 1—timescale derived from the rotation of the Earth
UTC	Coordinated Universal Time
UTC _r	rapid UTC

1. Introduction

International Atomic Time (TAI) was established by the Consultative Committee for the Definition of the Second (CCDS) in [1] after the adoption of the atomic definition of the second by the 13th General Conference on Weights and Measures (CGPM) in [2, 3]. The practical, disseminated reference time scale Coordinated Universal Time (UTC), based on TAI, is equally stable and accurate as TAI, but while TAI is continuous, UTC is affected by one-second discontinuities, known as leap seconds, as a consequence of its definition adopted in [4].

The progress in time and frequency metrology, physical sciences and industry impacted on the evolution of UTC. This article will review the history of the development of UTC in parallel with the scientific milestones that have been achieved to reach its present status.

The algorithm for the calculation of TAI/UTC has been designed to guarantee the reliability, long-term frequency stability, high frequency accuracy and accessibility of the time scale. It relies on clock readings and is highly dependent on the quality of the clock comparisons. The BIPM, in a coordinated effort with the world timing community, is dedicated to developing and improving these methods.

The number of atomic clocks and its variety has dramatically increased in recent years (there are almost 420 today), making it necessary to adapt the algorithms to make their best use in the quest for the optimum stability of UTC. Also, the methods and procedures for time and frequency transfer have developed significantly, allowing the comparison of the best atomic clocks without degrading their accuracy. Advances in the construction and operation of very accurate frequency standards, together with the improvement of methods for their comparison, are challenging metrologists to work towards a new definition of the SI second.

The BIPM assures the dissemination of UTC through *Circular T*; it is published monthly and today offers complete information for the benefit of National Metrological Institutes (NMIs), observatories and international organizations that contribute to its computation.

This review also describes other time scales maintained by the BIPM for various applications; a yearly realization of terrestrial time (TT(BIPM)), and the weekly rapid realization of UTC (UTC_r). Additional time scales are used for the computation of UTC as reference for parameters optimization. The paper concludes with a discussion on the perspectives for further developments on UTC.

An important aspect of UTC concerns its role in the framework of the CIPM MRA. After the implementation of CIPM MRA in 1999, the time came in 2006 for the CCTF to decide that the unique key comparison (KC) in the time and frequency field is that corresponding to the computation of UTC by the BIPM, and called it ‘CCTF-K001.UTC’. UTC is the key comparison reference value, and the degrees of equivalence of participants ‘*k*’, namely [UTC–UTC(*k*)] are available at the key comparison data base (KCDB) every month, after the publication of BIPM *Circular T*.

In figure 1 a scheme of the different time scales and their relations is reported to help the understanding of the paper.

2. The history of UTC

The 13th CGPM decided in [2, 3] that the second is the duration of 9 192 631 770 periods of the radiation corresponding to the transition between two hyperfine levels of the ground state of the caesium 133 atom [5]. It was later clarified that this definition refers to an atom at rest at a thermodynamic temperature of 0 K [6]. The recommendation of this transition for the definition of the time unit called for the adoption of a time scale built by accumulating atomic seconds. The unification of time on the basis of the atomic time scale already computed at the Bureau international de l’heure (BIH) was recommended by the International Astronomical Union (IAU) [7], the International Union of Radio Sciences (URSI, 1969) and the International Radio Consultative Committee of the International Telecommunication Union [8] (CCIR, 1970, predecessor of the Radiocommunication Sector of the International Telecommunication Union, ITU-R). Ultimate consecration came from the official recognition by the 14th CGPM in 1971 [9, 10], which introduced the designation ‘International Atomic Time’ and the universal acronym TAI.

TAI was then defined as ‘the time reference established by the BIH on the basis of the readings of atomic clocks operating in various establishments in accordance with the definition of the second’. In 1980 the definition of TAI was completed by the CCDS (renamed Consultative Committee for Time and Frequency, CCTF in 1997), adding ‘TAI is a coordinate time scale defined in a geocentric reference frame with the SI second as realized on the rotating geoid as the scale unit’. This definition explicitly refers to TAI as a coordinate time, recognizing the need of a relativistic approach. TAI is the basis of the realization of time scales used in dynamics, for modeling the motions of artificial and natural celestial bodies, with applications in the exploration of the solar system, tests of theories, geodesy, geophysics, and studies of the environment. In spite of the request of the CGPM to the CIPM in [9, 10] to provide a definition of TAI, a formal definition never arrived

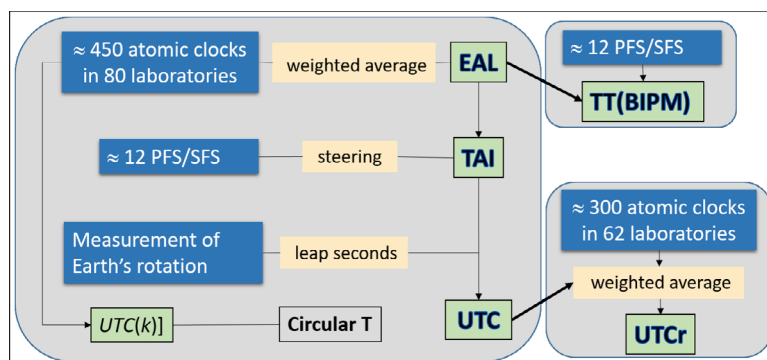


Figure 1. Representation of EAL, TAI, UTC, UTC(k), TT(BIPM) and their relations.

and in consequence there was at that time no definition of TAI and UTC made by the CGPM. This historical omission was addressed in 2017 with a proposal made by the CCTF of a set of formal definitions of the international time scales TAI and UTC [11] to be adopted as a resolution of the CGPM in November 2018.

Nevertheless, TAI was never disseminated directly and UTC, which was designed to approximate UT1 (a timescale derived from the rotation of the Earth), was chosen as the practical world time reference. The method for synchronizing UTC to UT1 was defined by the International Radio Consultative Committee of the International Telecommunication Union (CCRI); the use of UTC was endorsed by the 15th meeting of the CGPM in [12]. At the time of its definition, UTC was the unique means of having real time access to UT1, as needed for some specific applications including astronomical navigation, geodesy, telescope settings, space navigation, satellite tracking, etc. The definition of UTC is based on the atomic second, but the time scale is synchronized to UT1 to maintain $|UT1 - UTC| < 0.9$ s. Since 1972, UTC differs from TAI by an integral number of seconds, value that changes at the insertion of a leap second, which occurs as predicted and announced by the International Earth Rotation and Reference Systems Service (IERS). Since January 2017 and until further notice, the offset between TAI and UTC is 37 s.

Since 1988 the BIPM is responsible for the computation of TAI and UTC. An algorithm developed by the BIPM time department treats clock data submitted by institutes worldwide spread to give traceability to the SI second to the local realizations of UTC, named UTC(k) where k refers to a laboratory. The dissemination of the international time UTC by time and frequency signals is regulated by the ITU-R [13]; in parallel, Global Navigation Satellite Systems (GPS and GLONASS at present) provide the broadest dissemination of UTC. For a complete historical evolution of timescales see [14]. UTC is represented by local approximations identified as UTC(k) in laboratories 'k'. It is calculated in post-real time over one-month data batches, and is available monthly in the BIPM *Circular T* [15] under the form of values $[UTC - UTC(k)]$ at five-day intervals. Extrapolation of values over 10 to 45 days based on prediction models is necessary to many applications. UTC, as published today, is not adapted for real and quasi-real time applications and it was recognized that a more rapid realization would benefit:

- UTC contributing laboratories with more frequent assessing of the UTC(k) steering, and consequently better stability and accuracy of UTC(k) and enhanced traceability to UTC;
- users of UTC(k) with access to a better local reference, and indirectly, better traceability to the UTC global reference;
- users of Global Navigation Satellite Systems (GNSS) would get a better synchronization of GNSS times to UTC, through improved UTC and UTC(k) predictions: this is the case of UTC(USNO) for GPS, UTC(SU) for GLONASS, and of the UTC(k) to be used in the generation of Galileo, BeiDou and IRNSS/Gagan system times.

These reasons resulted in the BIPM to implementing UTCr (rapid UTC) [16] in July 2013, a new realization of UTC available with a shorter delay than *Circular T*. UTCr is a weekly solution based on daily data covering four consecutive weeks, reported daily by contributing laboratories. It is disseminated through daily values of $[UTCr - UTC(k)]$ published at one-week intervals on the Wednesday afternoon, providing access to results up to the preceding Sunday.

3. Properties of time scales

The phenomenon taken as the basis of a timescale should be reproducible with a frequency that is, ideally, constant. This is never exactly the case, so we must be able to identify the causes of its variation, and to eliminate or at least minimize them. The realizations of the second of the International System of Units (SI) [17] differ from the ideal duration specified in its definition (where the hyperfine splitting of the caesium 133 atom, at rest at a temperature of 0 K, is 9 192 631 770 Hz); in the process of constructing a timescale we should be capable of reducing these differences.

The reliability of a timescale is closely linked with the reliability of the clocks whose measurements are used for its construction; at the same time, redundancy is also required. In the case of the international reference timescale, a large number of clocks are needed; this number is today about 420, most of which are high-performance commercial caesium atomic standards and active hydrogen masers.

The frequency stability of a timescale represents its capacity to maintain a fixed ratio between its unitary scale interval and its theoretical counterpart.

The frequency accuracy of a timescale represents the aptitude of its unitary scale interval to reproduce its theoretical

counterpart. After the calculation of a timescale on the basis of an algorithm conferring the required frequency stability, the frequency accuracy can be improved by comparing the frequency (rate) of the timescale with that of primary frequency standards (PFS) or another more accurate time scale taken as a reference (for ex. most UTC(k) are steered to UTC; GNSS times are steered to a local UTC(k)), and by applying, if necessary, frequency (rate) corrections.

The accessibility to a world-wide timescale represents its aptitude to provide a way of dating events for everyone. This depends on the precision that is required. We consider here only the ultimate precision, which necessitates an observation of a few tens of days for reducing time transfer noise and profiting from the stability of the participating clocks. The long-term frequency stability required for a reference timescale in such a way is reached. Moreover, the process needs to be designed in such a way that the measurement noise is eliminated or at least minimized; this requires a minimum number of data-sampling intervals.

The instability of TAI, estimated today as three parts in 10^{16} for averaging times of about 30 d, is obtained by processing clock and clock comparison data at 5 d intervals over a monthly analysis, with a delay to publication of less than ten days after the last date of data reported in the official document called BIPM *Circular T* [15]. In the very long term, over a decade, the stability is equivalent to the accuracy maintained by PFS and is therefore at the level of 7 or 8 parts in 10^{16} considering the performance of the past decade.

4. UTC calculation

Different algorithms can be considered depending on the requirements of the scale. For an international reference such as UTC, the requirement is extreme reliability and long-term frequency stability. UTC therefore relies on the largest possible number of atomic clocks of different types, located in different parts of the world and connected via a network that allows precise time comparisons between remote sites. Each month the differences between the international time scale UTC and the local time scales UTC(k) maintained at the contributing time laboratories are reported at 5 day intervals in an official document called BIPM *Circular T* [15]. The various time laboratories worldwide achieve a stable local time scale based on individual atomic clocks or a clock ensemble. The clock readings reported by these laboratories are then combined at the BIPM through an algorithm designed to optimize the frequency stability and accuracy as well as the reliability of the time scale beyond the level of performance that can be realized by any individual clock in the ensemble. The BIPM time department uses an appropriate algorithm [18–25] to generate the international reference UTC each month. The calculation of UTC is carried out in three steps:

- The free atomic time scale EAL is computed as a weighted average of about 420 free-running atomic clocks distributed world-wide. A clock weighting procedure has been designed to optimize the long-term frequency stability of the scale.

- The frequency of EAL is steered to maintain agreement with the definition of the SI second, and the resulting time scale is TAI. The steering correction is determined by comparing the EAL frequency with that of the PFS/SFS.
- Leap seconds are inserted to maintain agreement with the non-uniform time derived from the rotation of the Earth. The resulting time scale is UTC.

The general equation of EAL is defined as follow:

$$\text{EAL}(t) = \sum_{i=1}^N w_i [h_i(t) + h'_i(t)] \quad (1)$$

where N is the number of atomic clocks, w_i the relative weight of the clock H_i , $h_i(t)$ is the reading of clock H_i at time t and $h'_i(t)$ is the prediction of the reading of clock H_i to guarantee the continuity of the time scale. The weight attributed to a given clock reflects its long-term stability, since the objective is to obtain a weighted average that is more stable in the long term than any of the contributing elements [23, 26].

The weights of the clocks obey the relation:

$$\sum_{i=1}^N w_i = 1. \quad (2)$$

Subtracting the same quantity from both sides of equation (1),

$$\text{EAL}(t) - \sum_{i=1}^N w_i h_i(t) = \sum_{i=1}^N w_i [h_i(t) + h'_i(t)] - \sum_{i=1}^N w_i h_i(t). \quad (3)$$

Using equation (2) and rearranging,

$$\sum_{i=1}^N w_i (\text{EAL}(t) - h_i(t)) = \sum_{i=1}^N w_i h'_i(t). \quad (4)$$

Setting

$$x_i(t) = \text{EAL}(t) - h_i(t), \quad (5)$$

it is clear that equation (4) is of the form

$$\sum_{i=1}^N w_i x_i(t) = \sum_{i=1}^N w_i h'_i(t). \quad (6)$$

Adapted algorithms will be used for the weights and for the prediction and they will be presented in detail in the next sections. The data used take the form of time differences between readings of clocks, written as:

$$x_{ij}(t) = h_j(t) - h_i(t). \quad (7)$$

Equation (6) in conjunction with the $N - 1$ equation (7) results in a system with N equations and N unknowns:

$$\begin{cases} \sum_{i=1}^N w_i x_i(t) = \sum_{i=1}^N w_i h'_i(t) \\ x_i(t) - x_j(t) = x_{ij}(t). \end{cases}$$

The solution is:

$$x_j(t) = [\text{EAL}(t) - h_j(t)] = \sum_{i=1}^N w_i [h'_i(t) - x_{ij}(t)]. \quad (8)$$

The difference between any clock H_j and EAL depends on weights, clock prediction and measured clock differences.

The clock H_j may also represent a UTC(j) time scale; therefore, $x_j(t)$ may also be interpreted as $x_j = \text{EAL} - \text{UTC}(j)$ having dropped the time instant t in the notation for simplicity.

5. The essential components of UTC calculation

This section describes how the clock, time transfer and PFS/SFS data (the basic ingredients of UTC calculation) are used for achieving a time scale with the properties requested to UTC as long term frequency stability and accuracy. The number of atomic clocks has progressively increased over time; the ensemble consists today of 52% high performance caesium clocks, 25% hydrogen masers and five rubidium fountains. The algorithms which model the clock frequency behavior and weights are designed to profit at best the metrological quality of the clocks. As presented in section 4 the atomic clocks are introduced in the computation of UTC through the difference of their readings. Improving clock comparison is a key factor in the quality of UTC because the dominant noise of the short-term stability of UTC is the time transfer noise.

5.1. The algorithms

A key point for UTC conception is the development of algorithms studied for using clock and time transfer data for achieving the best metrological properties requested to UTC that are long-term stability and accuracy. Considering the general description of UTC calculation made in section 4 it is possible to conclude that the prediction and weighting algorithms are the base for the stability requested to EAL and the steering algorithm for maintaining the frequency of UTC close to the SI definition of the second. Another algorithm considered in this section concerns the uncertainty of [UTC–UTC(k)] as reported in section 1 of *Circular T*. In the following subsections these algorithms will be presented with all the necessary details.

5.1.1. Prediction algorithm. In this section we present the clock frequency prediction algorithm currently used in the calculation of UTC. The algorithm for the atomic clock frequency prediction has been updated in [22] by introducing the quadratic model in phase data for the atomic clocks. This method is based on a quadratic model for describing the frequency drift of the H-masers or the ageing of the caesium clocks. Considering two successive intervals of UTC calculation, $I_{k-1}(t_{k-1}, t_k)$ and $I_k(t_k, t_{k+1})$ we impose several conditions on the prediction term $h'_i(t)$ at time t_k to avoid or minimize time and frequency jumps in the resulting time scale. The prediction term $h'_i(t)$ can be expressed as the following quadratic form:

$$h'_i(t) = a_{i,I_k}(t_k) + y_{ip,I_k}(t)(t - t_k) + \frac{1}{2}C_{ip,I_k}(t)(t - t_k)^2. \quad (9)$$

To evaluate the parameters in (9), that are the phase, the frequency and the frequency drift of the atomic clocks, we assume that at time t_k the following conditions exist on h'_i :

1. no time steps, by imposing the continuity to EAL;
2. no frequency steps, by imposing the continuity to the first derivative of EAL;
3. no change in frequency drift, by imposing the continuity to the second derivative of EAL.

We obtain a system of three equations with three unknowns and by solving this system we find that the relation (9) can be expressed as:

$$\begin{aligned} \hat{h}'_i(t) &= \hat{a}_{i,I_k}(t_k) + \hat{y}_{ip,I_k}(t - t_k) \\ &+ \frac{1}{2}\hat{C}_{i,I_{k-1}}(t_k - t_{k-1})(t - t_k) + \frac{1}{2}\hat{C}_{ip,I_k}(t - t_k)^2. \end{aligned} \quad (10)$$

The physical meanings of the terms present in (10) are:

- \hat{a}_{i,I_k} is the estimation of the time correction relative to EAL of clock H_i at date t_k
- \hat{y}_{ip,I_k} is the estimation of the frequency of clock H_i , relative to EAL, predicted for the period $[t_k, t]$
- \hat{C}_{ip,I_k} is the estimation of the frequency drift of the clock H_i , relative to a frequency reference, predicted for the period $[t_k, t]$
- $\hat{C}_{i,I_{k-1}}$ is the estimation of the frequency drift of the clock H_i , relative to a frequency reference, for the period $[t_{k-1}, t_k]$.

Considering that $\hat{C}_{i,I_{k-1}}$ is equal to \hat{C}_{ip,I_k} the prediction takes a more simple form:

$$\begin{aligned} \hat{h}'_i(t) &= \hat{a}_{i,I_k}(t_k) + \hat{y}_{ip,I_k}(t - t_k) \\ &+ \frac{1}{2}\hat{C}_{ip,I_k}(t_k - t_{k-1})(t - t_k) + \frac{1}{2}\hat{C}_{ip,I_k}(t - t_k)^2. \end{aligned} \quad (11)$$

The physical assumptions described in the relation are the constant drift and the variability of the frequency of each clock in the ensemble during the calculation interval.

Parameter estimation. The relationship (11) describing the correction applied to the atomic clocks includes three parameters, the phase, the frequency and the frequency drift. A major issue is the optimization of the estimation procedure. In particular the estimation of the frequency drift requires special attention. The estimation of the time correction $a_i(t_k)$, added to avoid time jumps, is given by the last known point of the difference between EAL and each clock and is expressed as:

$$\hat{a}_{i,I_k}(t_k) = \text{EAL}(t_k) - h_i(t_k) = x_i(t_k). \quad (12)$$

From a theoretical point of view the best estimation of the mean frequency y_{ip,I_k} is the difference between the last and the first point on the interval duration of the clock data with respect to EAL as expressed by the following relationship:

$$\hat{y}_{ip,I_k} = \frac{x_i(t_{k+1}) - x_i(t_k)}{t_{k+1} - t_k}. \quad (13)$$

To estimate the frequency drift of the ensemble of the clocks under the hypothesis that this drift remains constant on a one month interval, the choice of the frequency reference is very important. While the phase data ($EAL - h_i$) have been used to estimate the time and frequency corrections, the frequency data of the clock with respect to terrestrial time (TT) as realized by the BIPM TT(BIPM) [27, 28] (shortly reported as TT in the relationships), y_{TT-h_i} are used to estimate the drift. In details, the calculation of the drift of the ensemble of atomic clocks is obtained by applying the linear least square technique to the values of y_{TT-h_i} over three months. In the procedures described the biggest impact on the estimation of the drift is given by the choice of the frequency reference (TT(BIPM)) and the choice of the length of the evaluation interval:

- In [22] the use of EAL as a reference for frequency drift estimation has been tested showing that an external, very stable time scale is essential for having a satisfactory estimate that is not affected by the instability of the reference. It has been decided to use TT(BIPM) (its algorithm will be presented below) calculated with the data of PFS/SFS provided by the time laboratories to the BIPM as frequency reference for drift estimation.
- Considering the length of the interval for the drift evaluation, three months are used since the last modification of the algorithm. Before this, the best estimation interval (used during two years) was considered of six months but a shorter period resulted a better choice to cope with the variations of the H-masers drift over time. Very probably an equal interval for the estimation of the frequency drift of all clocks is not the optimum solution, and some other strategy should be designed.

5.1.2. Weighting algorithm. In this section the weighting algorithm as currently used in UTC calculation is presented [24]. The weighting algorithm was updated in 2014 to take in to account the frequency prediction model of the atomic clocks. The objective is to obtain a weighted average that is more stable in the long term than any of the contributing elements. In time-scale algorithms, clock weights are generally chosen as the reciprocals of a statistical quantity which characterizes their frequency stability, such as a frequency variance (classical variance, Allan variance, etc). The weighting strategy applied in UTC takes into account the prediction used in the calculation of EAL based on the principle that *a good clock is a predictable/stable clock* as used in other time scale algorithms [29, 30]. By using the EAL prediction the deterministic signatures affecting atomic clocks, such as the frequency drift or ageing, can be minimized or eliminated. H-masers are characterized by a very significant frequency drift that can usually be predicted with a very low uncertainty [31]. By taking into account this prediction the H-masers can contribute to the timescale ensemble with a realistic (significant) weight without degrading the long-term stability of EAL. This can be achieved by analyzing the difference between the frequency of the clocks y_{i,I_k} and their prediction

\hat{y}_{i,I_k} , obtained by using the relationship (11). Clearly the frequency drift of the H-masers must not be allowed to degrade the long-term stability of EAL. In UTC calculation an upper limit of weight is set to limit individual clock contributions to prevent domination of the scale by a small number of very stable clocks. The choice of a method to implement an upper limit of weight, as well as its value, thus plays an important role in the stability of the resulting time scale. The choice has been tested by the efficiency with which the stability of the scale is improved. The value is fixed equal to $w_{\max} = 4/N$ where N is the number of the clocks used in the calculation.

The principle behind the new weighting algorithm is that *a good clock is a predictable/stable clock*, by considering that in a time scale ensemble only the difference between the clock and its predicted value is used. During studies of the new prediction algorithm we observed that deterministic signatures such as frequency drift and ageing do not affect the EAL stability if well predicted. In the current procedure a four-iteration process is used where the weights are obtained by differencing the frequency with the predicted values. The differences between the predicted and the real frequencies are evaluated for each one-month interval over one year and these values are used to define the weight. By using one year's worth of data we maintain the long-term stability of EAL and UTC. In particular each iteration runs as follows:

1. The values $[EAL - h_i]$ are found using a given set of relative weights. In the first iteration, the weights are those obtained in the previous computation interval after normalization. In the following iterations, they are those obtained from the previous iteration;
2. The absolute value of the difference between the real frequency y_{i,I_k} and the predicted frequency \hat{y}_{i,I_k} obtained by the relationship (13) corresponds to:

$$\epsilon_{i,I_k} = |y_{i,I_k} - \hat{y}_{i,I_k}| \quad (14)$$

where the index i identifies the clock and I_k the time interval;

3. The square of (14) is evaluated for each clock;
4. One year of ϵ_{i,I_k} is considered to ensure long-term stability of EAL and UTC.
5. A filter has been implemented to give a more predominant role to more recent measurements with respect to older ones, considering that new measurements have most reliable statistics:

$$\sigma_i^2 = \frac{\sum_{j=1}^M \left(\frac{M+1-j}{M}\right) \epsilon_{i,j}^2}{\sum_{j=1}^M \left(\frac{M+1-j}{M}\right)} \quad (15)$$

where i identifies the clock, j the calculation interval and M the number of available measurements (which can vary from 5 to 12 given that 5 is the minimum number of months requested to observe the behaviour of a clock prior to its introduction into the UTC calculation and one year is the standard period of observation).

6. The relative weight of clock H_i is computed theoretically using a temporary value given by

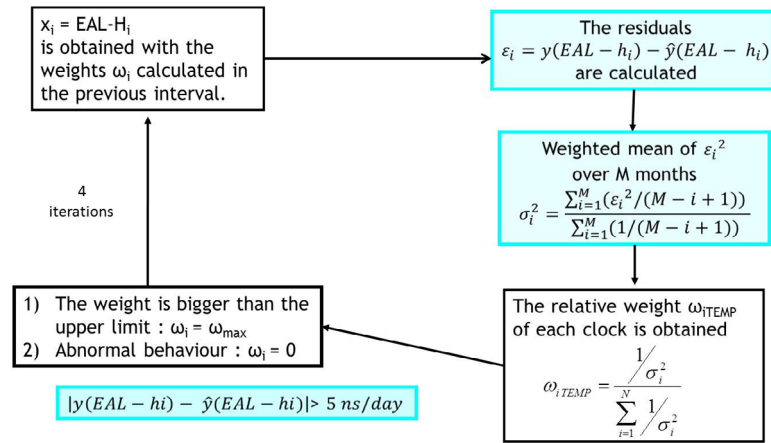


Figure 2. Iteration process for the weighting algorithm.

$$\omega_{i,temp} = \frac{1/\sigma_i^2}{\sum_{i=1}^N 1/\sigma_i^2}. \quad (16)$$

The new weight ω_i of clock H_i is equal to $\omega_{i,temp}$ except in two cases:

1. Clock H_i satisfies the requirement set for the limitation of weight as for the current algorithm.
2. Clock H_i shows abnormal behaviour during the interval of computation so it cannot contribute. In this case the current value of the difference between the real frequency and the predicted one is checked. If the value is greater than a fixed threshold (that means 5 ns d⁻¹ of difference between the prediction and the real data corresponding to about 150 ns at the end of calculation interval) the clock is temporarily excluded from the ensemble. In such a way we eliminate about 1% of the total number of clocks participating in UTC that is a good compromise between maintaining the largest possible number of clocks without negatively affecting the quality UTC.

The maximum weight put equal to $w_{max} = 4/N$ is a good compromise between the stability of EAL, the distribution of the weight among the laboratories and the conditions stated in [32] that are:

- that a minimum of, for example, 5%–7% of the clocks be at maximum weight and
- that a combined weight of clocks at maximum weight be at least 40% of the total weight.

In figure 2 the weighting algorithms is schematized.

In the design of the new weighting algorithm an important part is dedicated to the choice of the filter presented in (15). The simplest form by optimizing the long- and short-term stability of EAL was chosen. The use of different filters, as for example the exponential filter [29, 30] and the use of a different value for M (number of available measurements) were tested. The results did not show a significant improvement in EAL stability by changing these parameters in the filter.

5.1.3. Steering algorithm. Another algorithm used for maintaining the frequency of UTC close to the SI second frequency is the steering algorithm. TAI is a realization of TT, a coordinate time of a geocentric reference system. TAI gets its stability from some 420 atomic clocks kept in some 80 laboratories world-wide and its accuracy from a small number of PFS and SFS developed by a few metrology laboratories. The frequency of EAL is compared with that of the PFS/SFS using all available data, and a frequency shift (frequency steering correction) is applied to EAL to ensure that the frequency of TAI conforms to its definition. Changes to the steering correction are expected to ensure accuracy without degrading the long-term (several months) stability of TAI, and these changes are announced in advance in BIPM *Circular T*. The accuracy of TAI therefore depends on PFS/SFS measurements, which are reported more or less regularly to the BIPM. Data from several PSF/SFS are combined to estimate the duration of the scale unit of TAI [27, 28]. The algorithm used at the BIPM to estimate the duration of the scale unit of TAI [27, 28] combines the individual calibrations of PSF/SFS and calculates the frequency of the time scale during a given interval T (usually the month of calculation of *Circular T*). The features of TT as realized by the BIPM (TT(BIPM)) will be presented in section 7.

The calibrations of the PFS/SFS are usually referred to a local independent time scale. When using them to improve the accuracy of TAI, we should account for the transfer resulting from the local time scale to the reference time scale (in this case EAL), and for the transfer of the frequency measurements from the various calibration dates to the period of interest T . This is due to the fact that we calculate the frequency of EAL for the calculation interval T (corresponding to the month of calculation of *Circular T*) but the evaluation of PFS/SFS can have a different duration (starting from 5 d) and the measurements be in a different interval. For example, when a new PFS/SFS starts contributing to the *Circular T*, all the available past calibrations are taken into account even if their evaluation period does not correspond to the current calculation month of *Circular T*.

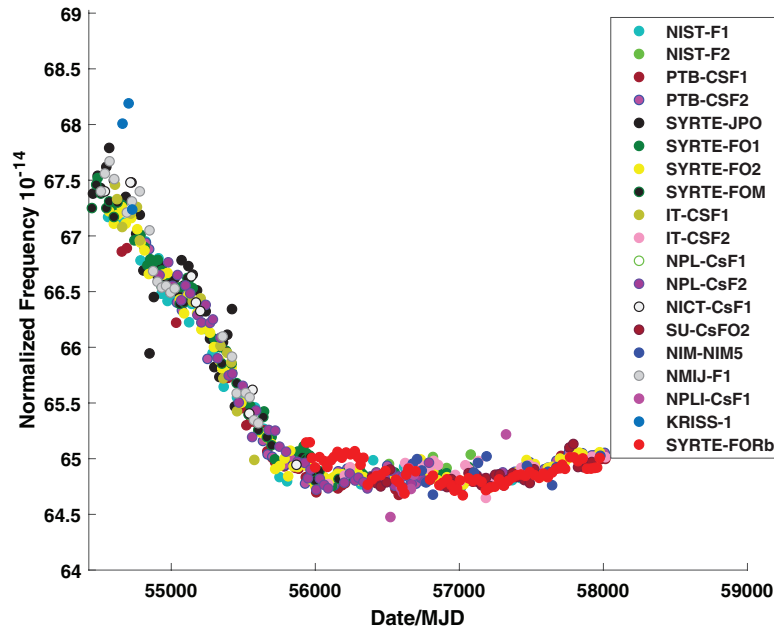


Figure 3. Comparison of the frequency of EAL with respect to PSF/SFS.

A frequency standard j carries out n_j calibrations. If N is the number of standards considered, the number of available calibrations will be $\sum_{j=1}^N n_j$. We calculate the rate of EAL over an interval T as:

$$y = \sum_{j=1}^N \sum_{i=1}^{n_j} a_{j,i} W_{j,i} \quad (17)$$

where $W_{j,i}$ is the rate difference between EAL and the PFS/SFS j for a given interval T_{ji} , and a_{ji} are the filter coefficients. The filter coefficients a_{ji} , are normalized and depend on:

1. the uncertainty of the evaluation i of the standard j (i is the index used for counting the number of evaluations of the standard j).
2. the distance between T_{ji} and T
3. the instability of EAL, which transfers the evaluation from T_{ji} to T .

In figure 3 the frequency of EAL is compared to PFS/SFS with the algorithm previously presented.

5.1.4. The uncertainty of UTC–UTC(k). The uncertainties of the differences between UTC and UTC(k) are published in section 1 of *Circular T* [33, 34]. They are affected by three major elements: clock variations, the means of comparisons of remote clocks (time transfer) and the time-scale algorithm. The analytical solution for the evaluation of the uncertainty of [UTC–UTC(k)] is based on the relation (8). In fact, as explained in section 4, the difference between EAL and the clock h_k (8) may also represent the difference between EAL and UTC(k) because H_k may also represent a UTC(k) and finally the difference between UTC and UTC(k). The three elements that could be source of uncertainty are the prediction, the weights and the time link differences. Considering the predictions and the weights fixed by appropriate algorithms and considered as time-varying deterministic parameters, the measures x_{ij} in

(7) are thus the only contributors to the uncertainties in x_j (8) and are the only source of the uncertainty of [UTC–UTC(k)]. The current algorithm [33, 34] applies the law of uncertainty propagation to (8) for obtaining the following solution for the uncertainty:

$$u_{x_k}^2 = \sum_{i=1}^N w_i^2 u_{x_{i,k}}^2 + 2 \sum_{i=1}^{N-1} \sum_{j=i+1}^N w_i w_j u_{(x_{i,k}, x_{j,k})} \quad (18)$$

where $u_{x_k}^2 = u_{\text{EAL}-h_k}^2$. The weights of the clocks are available from the BIPM website, and the uncertainties of links between the clocks are published in *Circular T* [15]. The second part of the equation (18), representing the correlation between clocks in different laboratories, is currently put equal to zero and consequently the clocks are considered uncorrelated. A revision of the algorithm is being studied and will be officially applied in the near future [35]. One of the most important difference, with respect to the current method used for the calculation of uncertainties is the introduction of the correlations. The evaluation of the correlations is generally a complex procedure and actions could be envisaged for their evaluation. The most important consideration concerns the distinction between the two main techniques of remote clock comparison (GNSS and TWSTFT) used for UTC generation. In fact the result of a GNSS calibration can be associated to the laboratory's receiver while the calibration of TWSTFT measurements characterizes the links. Based on this physical assumption the GNSS time links will be considered with respect to an auxiliary time scale (ATS) instead of UTC(PTB). Being ATS external to UTC calculation (this is not the case of UTC(PTB) in the current UTC structure) the evaluation of correlations is possible. For the TWSTFT time links, the PTB laboratory will remain the pivot, even if in the case of redundant time links all the possible TWSTFT measurements should be considered. The formalism used and considered in [35] will be finalized for describing this physical reality.

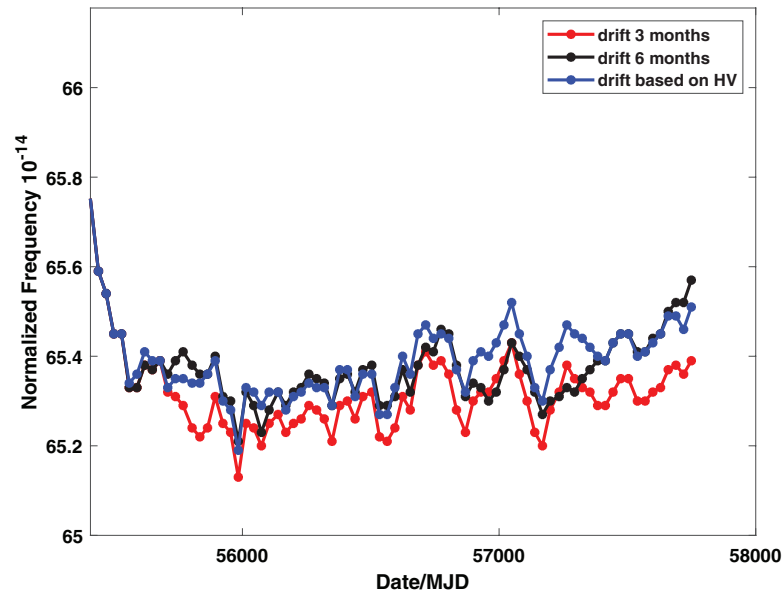


Figure 4. Frequency of EAL with respect to PSF/SFS calculated by evaluating the frequency drift with 6 (black line), 3 (red line) and optimized period (blue line) are compared.

5.2. The future development of time scale algorithms for UTC calculation

Further improvement to the algorithm for the calculation of UTC is under study. Two different approaches are being considered; the evolution of the current method, correcting the weakness that has emerged from many years of experience treating each clock in a independent way, and a completely new approach using the Kalman filter. A combination of the current method with the Kalman filter tool could be an ideal solution for UTC.

5.2.1. Single atomic clock analysis. In order to assess the progress with the current algorithm for UTC we have started studies on individual clocks. In particular, the interval for the evaluation of the frequency drift of each clock, that is currently three months, could be considered depending on the stability property of the atomic clocks. This could lead to the use of different intervals of estimation for each clock. A test has been done by considering three years of atomic clock data with respect to TT(BIPM). The Hadamard Variance is calculated for the data (TT-Hi) (3 years), its minimum value corresponds to the optimized interval for the i th clock (the longer predictable period for the drift estimation). The results show that 15% of the clocks are very predictable and the best drift evaluation interval is 6 months. For the rest of the clocks, 3 months is the longer predictable period. In the future the characterization of each single clock with respect to its drift predictability will be developed to rapidly detect clock anomalies and prevent their negative impact on UTC.

In figure 4 the frequency of EAL with respect to PFS/SFS calculated by evaluating the frequency drift with 6 months (black line), 3 months (red line) and optimized period (blue line) are compared. In figure 5 the Allan deviation of the previous data is reported.

5.2.2. Kalman filter time scale. A Kalman filter time scale has been tested to improve the performance of UTC [36]. The Kalman filter is used in many fields because of its ability to clean data with white phase noise. In the time and frequency domain, use of the Kalman filter is especially important because of its use in building time scales. The short-term stability of UTC is dominated by the white noise of time transfer used to compare clocks; the idea is to improve UTC stability by means of the Kalman filter. A typical example of real-time time scale build with the Kalman filter algorithm is IGS (international GPS service time scale) [37]. In this first stage of the test an ensemble of 139 atomic clocks having run continuously without time and frequency steps for 3 years has been selected. UTC is calculated with this ensemble of clocks. The Kalman-based time scale is calculated by using the weights automatically obtained by the Kalman routine and the results are compared to those acquired by using the weights obtained from the UTC algorithm; the main difference between the ensemble of weights is the maximum weight fixed in UTC algorithm and not implemented in the classical Kalman filter routine.

EAL₁₃₉ (calculated by using 139 atomic clocks) is less stable than the current time scale but the quality is sufficiently good to be used for the test. We should observe that the parameters (frequency of the clocks, frequency drift etc) are optimized for having a long-term time scale in the case of 450 atomic clocks. Different choices should be made in the case of about 150 atomic clocks. However the results are good enough for the scope of our first analysis. The input data for our computation was therefore of the form $EAL_{139} - h_i$ with $i = 1, \dots, 139$. From that, we estimated the clock parameters (initial state and noise coefficients) attributing the whole noise signature to the h_i . The noise coefficients are calculated by comparing the clocks to TT(BIPM) and by performing the Hadamard variance. Before analysing this comparison there is another aspect on which we need to focus our attention: the

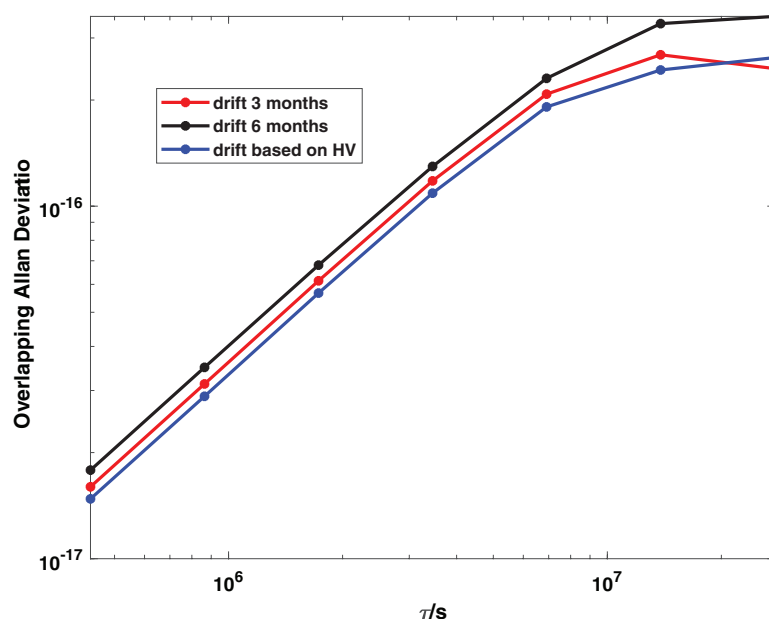


Figure 5. Allan deviation of the previous data.

clock weights. The x -reduction procedure in the case of measurement noise delivers, together with Kalman's estimates, a weight for each laboratory, based solely on the clock stability. However this kind of weight does not suit our purposes as it does not introduce a maximum for each clock weight (thus affecting the reliability of the scale). In this case the weights are completely dominated by the Rubidium fountains, as their stability is much better than those of the other clocks. Therefore we use the EAL weights for our computation, based, and previously described, on the principle that *a good clock is a predictable clock*. Figure 6 shows the stability comparison between EAL, the KF scale with EAL weights and the KF Scale with Kalman weights all with respect to a Rubidium fountain. We can observe that the KF Scale shows an improved stability with respect to EAL, particularly in the case of Kalman weights. This is not surprising as not having a maximum weight constraint implies that the scale can rely only on the better performing clocks. This fact, even if it allows a better stability, makes the scale much less robust to possible problems that can affect these high performance clocks.

5.3. The time transfer applied to clock comparisons

The calculation of a timescale on the basis of the readings of clocks located in different laboratories requires the use of methods of comparison of distant clocks. A prime requisite is that the methods of time transfer do not contaminate the frequency stability of the clocks; in fact in the past they were often a major limitation in the construction of a timescale.

UTC is built with the contribution of 80 laboratories more or less well spread over the planet; therefore a strategy for the clock comparison, consistent with the designed algorithm, needs to be well defined. Based on the principle of non redundant comparisons, the BIPM establishes a network of international time links which consists, as of beginning of 2018,

in a star-like scheme that links all contributing laboratories to a unique pivot, currently the Physikalisch-Technische Bundesanstalt (PTB) in Germany. As a consequence of the variety of methods of time transfer operated in laboratories, the pivot has been selected among those laboratories equipped with, and running on a continuous basis, all time transfer methods. This condition is fulfilled by several laboratories, giving the possibility of changing the pivot in case of technical need.

The statistical uncertainty of clock comparison ranges today from a few tenths of nanosecond to a nanosecond for the best links, *a priori* sufficient to allow a comparison of the best atomic standards over integration times of a few days. This assertion is strictly valid for frequency comparisons, where only the uncertainty of the random fluctuations affects the process. In the case of time comparisons, the uncertainty coming from the calibration of time transfer equipment operated in laboratories must also be considered. In the present situation, calibrations contribute an uncertainty that exceeds the component of the random fluctuations, and which can reach an undetermined number of nanoseconds for non-calibrated equipment. It can be inferred that repeated measurements of the equipment signal delay are indispensable for clock comparison.

The participating laboratories provide time transfer data in the form of a comparison of their UTC(k) with respect to another timescale—currently the internal time scale of a global navigation satellite system (GNSS)—or to another local realization of UTC, as in the case of two-way satellite time and frequency transfer observations. A section of this paper 5.4 will be dedicated to calibration work and to the estimated uncertainties.

5.3.1. Use of GNSS for time transfer. Time transfer is possible using the signal broadcast by GNSS satellites, which contains timing and positioning information. It is a one-way

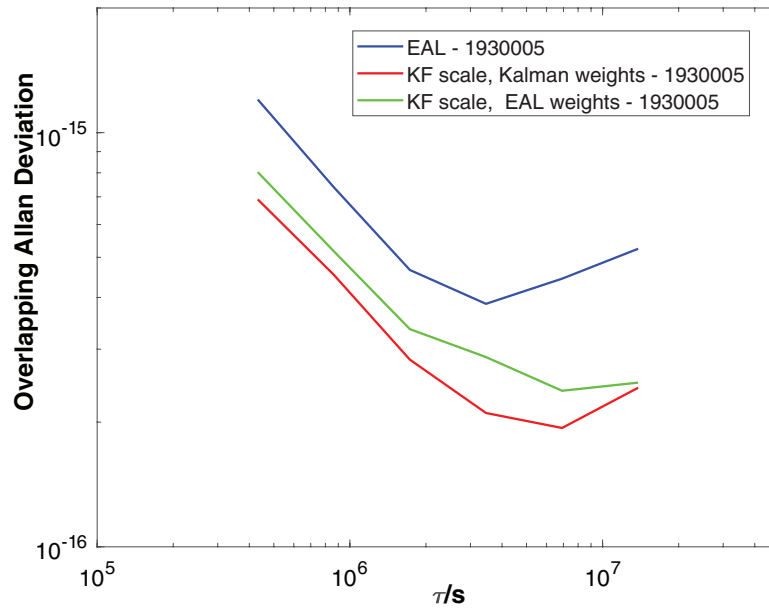


Figure 6. Stability comparison of EAL-1930005 (higher line), the KF scale -1930005 with EAL weight (middle line) and the KF scale -1930005 with Kalman weights (bottom line).

method, the signal being emitted by a satellite and received by specific equipment operated in a laboratory. For this purpose, GNSS receivers have been developed and commercialized to be used specifically for time transfer. This first generation of receivers evolved from single-frequency, single-channel to single-frequency, multi-channel. In the early 2000s the use of geodetic-type receivers had been studied and validated; it became possible implementing externally to the receiver the time comparison with the laboratory clock. They had the advantage of performing dual frequency measurements, thus correcting the ionospheric delays. The interaction of time metrology experts with GNSS receivers developers resulted in the conception of receivers specific for time comparisons which incorporate the geodetic-type receivers advantages. The text below explains the progress achieved with this equipment [38]. The common-view (CV) method [39] relies on the reception by several receivers of the same emitted signal. GNSS time transfer is intrinsically affected by the position errors of the satellite and by the instability of the satellite clock. These effects are eliminated or minimized when the two stations involved in the clock comparison observe the same satellite simultaneously. The CV method requires simultaneous observation of satellites at the two stations, with the drawback that with increasing distance the number of simultaneously observed satellites decreases, and the number of high elevation satellites becomes poor. Common-views of satellites of the US global positioning system (GPS) were used for the calculation of UTC at the BIPM until 2006.

The observation equation [40] for the GPS common view method between receivers i and j is given as:

$$P_i^k - P_j^k = \rho_i^k - \rho_j^k + I_i^k - I_j^k + T_i^k - T_j^k + c(dt_i - dt_j) + e_i - e_j \quad (19)$$

where k is the satellite pseudo-random noise (PRN) number and ρ is the geometric distance between the satellite antenna

and receiver antenna. Here, I represents ionospheric refraction delay and T is tropospheric refraction delay, dt is the difference between the satellite time and the local clock, and e is measurement error including multi-path effects and the delay in the receiver. Because P is the observation value, and I and T are derived from the GPS navigation message and measurement error, $(e_i - e_j)$ is assumed to be 0; so we can obtain the time difference $(dt_i - dt_j)$.

Then advances in obtaining precise satellite orbits and clock parameters allowed the introduction of another technique, named All in View (AV) [41] that eliminates the constraint of having simultaneous observations, thus becoming independent of the length of the baseline for having suitable observed satellites. In AV, data from all satellites in view at a station are used. The International GNSS Service (IGS) has provided since 2004 high precision GPS satellite clock products referred to the timescale of the IGS (IGST) [37], which relative frequency instability is of order 10^{-15} for a one-day averaging time, two orders of magnitude better than that of the GPS time. Since this minimizes the impact of the error coming from satellite orbits and clocks, it has been possible to use the AV method instead of the GPS CV with the benefit of adding data from satellites at high elevations and thus improving the statistical uncertainty of the time links, particularly the very long ones [41]. The GPS links obtained using dual-frequency receivers, termed GPS P3 [38, 42], provide ionosphere-free data and allow clock comparisons with nanosecond statistical uncertainty or better. The delay imposed by the ionosphere to the electromagnetic signals is one of most difficult to model accurately. Dual-frequency receivers perform simultaneous measurements in two frequencies (f_a and f_b) and eliminate almost completely first order ionospheric effects by a linear combination of the measurements M_a and M_b (code or phase) at the two frequencies, as in the simple equation:

$$M_{I-free} = \frac{f_a^2 M_a - f_b^2 M_b}{f_a^2 - f_b^2}. \quad (20)$$

In a GPS P3 link only code measurements are used. Most remaining error sources are under 0.1 ns, the precision with which TAI is reported. Code-multipath effects can reach 1 ns on a short-term basis and higher values in the long term, representing the ultimate limit to code-only time transfer either with CV or AV. Tropospheric delay is still present in the data, introducing short-term noise and bias of a few 0.1 ns, with slow variations depending on weather conditions. The addition of phase measurements from geodetic-type receivers minimizes the effects of these two error sources. The precise positioning technique (PPP) [43, 44] in which dual-frequency phase and code measurements are used for comparing via GPS the reference clock in a station to a reference timescale has been implemented for use in the computation of time links for UTC and has been used on a routine basis since September 2009. By this technique we obtain the smallest statistical uncertainty of clock comparison, at present about 0.3 ns.

Two time transfer data protocols are accepted at the BIPM for data submission. For the code measurements, a special format and procedure for data tracking and averaging had been developed in 1994 for GPS [45] by the CCTF Group on GPS Time Transfer Standards, commonly known as ‘CGGTTS format’ and extended later to support GLONASS observations. These directives evolved with the income of new satellite systems, and its last version, CGGTTS version 2E [46] supports data from all GNSS fully and partially operational today. For the time comparisons using the phase of the signal combined with the code (presently the GPS PPP solutions) is necessary to make use of the ‘Receiver Independent Exchange Format’ RINEX, originally developed for geodetic applications. Its latest version, RINEX 3.03 [47] supports multi constellation data, including global (GPS, GLONASS, Galileo and BeiDou) and regional (Japanese QZSS and Indian IRNSS) satellite systems.

Thanks to new hardware and to improvements in data treatment and modelling, the uncertainty of clock synchronization via GPS has been reduced from a few hundred nanoseconds at the beginning of the 1980s to below 1 ns today. Old single-channel, single-frequency C/A code receivers have been replaced in time laboratories by multi-channel receivers, which allow the simultaneous observation of all satellites over the horizon. The effects of ionospheric delay introduce one of the most significant errors in GPS time comparisons in particular in the case of clocks compared over long baselines. GPS observations with single-frequency receivers used in regular UTC calculations are corrected for ionospheric delays by making use of ionospheric maps produced by the IGS. Dual-frequency receivers installed in most participating laboratories allow the removal of the delay introduced by the ionosphere, thus increasing the accuracy of time transfer. All GPS links are corrected for satellite positions using IGS post processed precise satellite ephemerides.

Studies on the use of the Russian satellite system GLONASS for clock comparisons in UTC started at the BIPM since the early 1990s, but had slow progress into real

application due to the time elapsed before fully displaying the system satellites. The first GLONASS time link between the PTB and the Russian Institute of Metrology for Time and Space (VNIIFTRI) in Moscow (represented by the acronym SU in BIPM *Circular T*) was introduced in the computation of UTC by the end of 2009 [48]. After many years of limited operations with a small number of satellites, GLONASS constellation is now fully operational. In UTC, GLONASS observations have been processed in common-view only, and the resulting link is combined with that of GPS. Different from GPS, the GLONASS satellites do not all transmit the same frequency, and the signal delay in the receiver is different for each satellite group transmitting the same frequency, provoking the unresolved technical issue of having multiple frequency biases affecting the code measurements. Studies on the possible causes and effects of these biases [49] did not reach a clear conclusion, but showed that using the L1C code with the common-view technique they are no larger than the measurement noise. Defraigne *et al* [50] showed that combining GPS and GLONASS code and phase observations the PPP solution is comparable to that with GPS observations only. Furthermore, the combined solution improves when only GLONASS phase observations are included.

5.3.2. Two-way satellite time and frequency transfer (TWSTFT). The TWSTFT [51, 52] technique utilizes a telecommunications geostationary satellite to compare clocks located in two receiving-emitting stations. Two-way observations are scheduled between pairs of laboratories so that their clocks are simultaneously compared at both ends of the baseline. The two-way method has the advantage over the one-way method of eliminating or reducing some sources of systematic error, such as ionospheric and tropospheric delays, and the uncertainty in the positions of the satellite and the ground stations. The differences between two clocks placed in the two stations are directly computed.

The observation equation [40] for the time transfer by TWSTFT is written as follows:

$$T_i - T_j = \frac{1}{2}(dt_i - dt_j) + (e_i - e_j) + t_s \quad (21)$$

where t_s is a correction term for the path difference due to the Earth’s rotation (the Sagnac effect), T_i and T_j are the compared time scales, $(e_i - e_j)$ the measurement error and $dt_i - dt_j$ the time difference measured for stations i and j .

The first TWSTFT link was introduced into TAI in 1999. Since then, the number of laboratories operating two-way equipment has increased, allowing links within and between North America, Europe and the Asia-Pacific region. Until mid-2004, intervals of 5 min measurements were made on three days per week, which were not sufficient to give significant statistics for their use in TAI calculation. With the installation of automated stations in most laboratories, however, the TWSTFT link observations in TAI are now made every day at two-hour intervals with an uncertainty below 1 ns. However, this statistical uncertainty has been degraded by additional noise with a daily signature, the origin of which is not yet clear. We will discuss in the section 10.3 on the possibilities

for improvement. The TWSTFT time links are characterized by an excellent accuracy, coming from the long-term stability of the hardware and represented by a 1 ns calibration uncertainty.

The protocol for TWSTFT data exchange has been developed at the International Telecommunication Union (ITU) for use in multiple applications [53]. This protocol is used for the regular submission of TWSTFT data to the BIPM.

The number of institutes operating two-way stations for time comparisons remains small for a number of reasons. First, the high cost of the TWSTFT equipment, several times that of a GNSS receiver; second the complexity of its operation, and finally the fact that a satellite service provider is necessary for the transmission of the signals, involving additional cost and coordination with the other participating institutes. It has, however, the advantage of the easy treatment of the observations, since time comparisons are already computed in the ITU protocol, and the final solution is purely geometrical, and safe from corrections.

5.3.3. Time links in UTC, their comparison and combination. For two decades, GPS C/A-code observations have provided a unique tool for clock comparisons in UTC, rendering impossible any test of its performance with respect to other independent methods. The present situation is quite different; the introduction of the TWSTFT technique and the GLONASS observations have resulted in the opportunity of comparing the time links obtained with GPS techniques with those coming from the independent GLONASS and TWSTFT techniques, and making the system more reliable. In parallel, new GNSS receivers had been developed, and refined methods for treating their observations had been implemented. With the dual frequency receiver data and the provision of RINEX files, iono-free P3 links and code/phase measures solutions (PPP) are computed whenever possible [44]. This gives the BIPM the possibility of computing and comparing a redundant number of time links for some baselines, the best being used in the calculation of UTC and the others kept as backup. The time links and the results of time link comparisons are available on the BIPM ftp server [54].

Redundant links over a baseline can be combined to enhance the comparison of the clocks involved [55]. This approach has been in use at the BIPM since January 2011, with the introduction of combined GPS/GLONASS and TWSTFT/GPSPPP time links. The combination of TWSTFT and GPSPPP results in a link characterized by the accuracy of TWSTFT (u_B 1 ns) and the short-term stability of GPS PPP, at the sub-ns level [56].

Data from single channel receivers stopped in mid-2015. As of January 2018, 22% of the links in UTC are obtained using GPS single-frequency data, 70% of time transfer data is from dual frequency GPS receivers, from which 58% is used in GPS PPP solutions. The TWSTFT links represent only 12% of the time links, they are all combined with GPSPPP. The few time links computed with a combination of GPS and GLONASS have been temporarily interrupted.

5.4. Characterization of the relative delay of time-transfer equipment and evaluation of link uncertainties

The measurement of the signal path delay originating at the time transfer equipment is essential to the stability of UTC and to the accuracy of its dissemination. It represents the largest component of the time link uncertainty, and obviously it dominates the uncertainty of $[UTC-UTC(k)]$ as computed by the BIPM.

As described in detail in section 4, the basic data for the computation of UTC are clock differences. The contributing laboratories report their clock data to the BIPM together with the time transfer files from which the differences between two local realizations of UTC are computed, following a well established procedure. In consequence, relative calibration of the time transfer equipment is sufficient for the purpose.

The BIPM has organized, since 2014, relative calibration campaigns of GPS equipment in coordination with the Regional Metrology Organizations (RMOs). Before 2014, GPS calibration campaigns had been organized by the BIPM only [57, 58], but the increasing number of contributing institutes and the redundancy of equipment in some laboratories motivated this successful arrangement. To assure the consistency between calibrations made by the different groups in the various metrology regions, the BIPM has issued guidelines for GNSS equipment calibration [59]. The campaigns result in the determination of differential delays of GNSS time transfer equipment to compensate for the internal delays in the laboratories by comparing their equipment with traveling equipment. This cooperation has been established to complete the calibration of equipment in all the contributing laboratories and to maintain a process of periodic calibrations within two or three years. A group of laboratories, identified as ‘G1 laboratories’ in the calibration procedures, have been selected as regional nodes which provide the reference to the regional calibrations; as of today they are nine: three in EURAMET, one in COOMET, three in APMP, two in SIM. The cooperation is under organization at AFRIMETS and GULFMET. 80% of the laboratories operate calibrated GPS equipment, and thanks to the BIPM-RMOs coordination, 44% have participated in at least one in one calibration campaign since 2014.

The BIPM estimates the standard uncertainties u_{Stb} and u_{Cal} of all GPS time links in UTC [59]. The uncertainty u_{Stb} is evaluated by taking into account the level of phase noise in the raw data and all other effects with typical duration up to 30 days; u_{Cal} is the uncertainty of the calibration. Hardware instabilities provoke changes in the internal delay value; an additional uncertainty component takes into account the aging of the measures u_{Ag} , with values increasing progressively after two years of the latest calibration. Also link alignment corrections are applied whenever necessary if the time transfer equipment in a laboratory is changed, adding a 1 ns component to the link uncertainty [60].

A standard value of the calibration uncertainty u_{Cal} of 1.5 ns is assigned to GPS calibrations younger than two years provided by the BIPM. An arbitrary -unrealistic- value of 20 ns is assigned to non-calibrated equipment, but this situation should not continue in the long term. Table 1 shows time

Table 1. Time links between some UTC contributing laboratories and the PTB (Germany). The type of each link and the respective u_{Stb} and u_{Cal} uncertainty values are those published in section 5 of BIPM *Circular T 367* corresponding to July 2018.

Laboratory	Link type	u_{Stb}/ns	u_{Cal}/ns	u_{Ag}/ns
APL	GPSPPP	0.3	11.2	10.0
CAO	GPSMC	1.5	20.0	—
DTAG	GPS P3	0.7	2.8	1.3
OP	TWGPPP	0.3	1.2	0.6

links between some UTC contributing laboratories and the PTB (Germany). The type of each link and the respective u_{Stb} and u_{Cal} uncertainty values are those published in section 5 of BIPM *Circular T 367* corresponding to July 2018.

These uncertainty components are also valid for the TWSTFT links, with values representing the quality of the measurement and the stability of the hardware. But the calibration of the TWSTFT links is different; the laboratories organize calibrations of their TWSTFT equipment with the support of the BIPM and of the CCTF Working Group on TWSTFT [61–64]. The operational aspects of a TWSTFT calibration campaign are described in the document ‘TWSTFT calibration guidelines for UTC time links’ [65]. The process consists of a calibration of the link between two stations with traveling equipment provided by a private company. In spite of the quality of TWSTFT links, their stability is threatened by incidents related to the satellite, which is operated independently of the metrology community. Frequency changes occur rather often, undermining the calibration of the links. Pending the calibration of all stations in this way, two-way links in UTC, are if necessary, calibrated at the BIPM using the corresponding calibrated GPS link.

5.5. Future developments in time transfer: IPPP, optical fibre links and software-defined radio receivers

Some new time transfer techniques are now under development and hopefully will be regularly used for time comparisons in UTC soon. Progress can be reported on three different approaches, PPP with integer ambiguity resolution (IPPP) for GPS, software defined radio (SDR) receiver for TWSTFT, and completely different, the fibre links. The BIPM time department compares each month time link results obtained with the different techniques we report on below, and publishes the results on the ftp server [54]. Although not yet tested for future implementation in the construction of UTC, the stability of code-phase TWSTFT can be improved with carrier-phase measurements.

Experiments at several institutes operating the TW technique demonstrated 4×10^{-16} frequency instability at one day with carrier-phase measurements over a long baseline [66], and the potential capability on reaching 10^{-17} with hardware improvement [67].

5.5.1. IPPP. A new technique that has the potential to revolutionize clock frequency comparisons using GPS signals has

been developed by the BIPM time department in collaboration with colleagues from the Centre National d’Etudes Spatiales (CNES) and the Collecte Localisation Satellites (CLS). Signals of the global positioning system (GPS) have been used to compare clocks at a distance for decades. The best present technique of choice is precise point positioning (PPP), which provides the majority of the links used for UTC. Its performance for frequency comparisons is of the order a few parts in 10^{16} in 10 d, which is adequate for all commercial clocks, but insufficient to compare the best caesium or rubidium fountains, which claim an accuracy below 2×10^{-16} , not to mention the forthcoming optical frequency standards. One way to overcome the current limitations of GPS for clock comparisons is to base the results only on the phase of the transmitted signals and to explicitly account for the integer-cycle nature of the phase ambiguities that need to be resolved between the different arcs and satellites that are successively observed during the comparison. Developing this technique, called IPPP (PPP with integer ambiguity resolution), has been a topic of collaboration with colleagues at the CNES and the CLS over the last few years. The CNES and CLS teams constitute one analysis centre of the International GNSS Service (IGS), and they are developing specific IGS products needed for IPPP. In the framework of a post-doctoral position during 2013–2014, jointly funded by the BIPM and the CNES, the operational procedures for IPPP were developed that allowed several long-term tests to be carried out (comparisons over weeks to months). A joint publication with colleagues at the BIPM, CNES and CLS describes the work [68]. The most significant result compares IPPP to a 420 km optical-fibre time link in Poland, which is in continuous operation and which reports to the BIPM. As a result of the fibre link’s better accuracy, it was possible to demonstrate that the IPPP technique reaches, in about 5 d, a performance of 1×10^{-16} in comparing the frequency of two clocks and that the achieved accuracy continues to improve with longer averaging times [54]. This represents a significant improvement over classical PPP and is the best published performance for a GPS frequency comparison. Because IPPP can compare two clocks whatever their locations on Earth and can be operated immediately with existing equipment, it will be a significant step towards the comparison of ultra-accurate clocks. Optical fibre links will progressively build up into networks that cover more extended continental areas, particularly in Europe. For world-wide frequency comparisons at the sub- 10^{-16} level we could refer to [69] and to atomic clock ensemble in space (ACES) mission [70, 71], which is expected to fly on board the International Space Station in 2020.

5.5.2. Fibre links. The optical fibre link (OFL) techniques have grown fast. Over thousands of kilometres, a coherent fibre link can compare clocks with an uncertainty of few parts in 1×10^{18} in 1000–10000 s. Also time transfer over fibre reports large advances, and today it can offer a sub-ns inaccuracy. Nonetheless, only two time links in Europe (AOS-GUM and BEV-TP) regularly report data to the BIPM connecting remote atomic clocks. The implementation of fibre

links reporting data to the BIPM shall be encouraged and pursued to take advantage of a widespread optical fibre network.

Fibre links comparisons demonstrated to be the currently most suitable means to compare remote optical frequency standards. More comparisons shall now be realized in order to achieve the target identified in the roadmap for the possible redefinition of the SI second, collecting more and more comparisons of optical frequency standards with an uncertainty of parts in 10^{18} . Nonetheless, there are not projects planned for an intercontinental fibre link. In the next years, the remote intercontinental comparison of optical frequency standards will become an issue. Intercontinental fibre links could be a possibility, but probably the use of advanced satellite techniques will be investigated and pursued to compare optical frequency standards at the right level of accuracy and stability.

Europe has, in 2018, the most extended network of fibre connections relying metrology institutes and research institutions where optical clocks are operated or in development. Microwave standards (Cs and Rb standards) operated at the national metrology institutes in France and Germany had been compared with a few 10^{-16} uncertainty [72]. With the support of EURAMET, projects have been put in place for optical-clock comparison with the target of operating long-distance optical links continuously with measurement uncertainty better than 10^{-17} over one day. Progress has also been made in Japan, relying institutes in the Tokyo area for remote comparisons of optical and microwave frequency standards [73].

5.5.3. SDR. The software-defined radio (SDR) receiver [74–76] has been developed at the Telecommunications Laboratory (TL, Chinese Taipei) for implementation in TW Earth stations. It is aimed at improving the stability of TW time transfer, with particular impact on the diurnal signature present in almost all the links, which is the major uncertainty source in TW time links. The BIPM and the Consultative Committee for Time and Frequency (CCTF) Working Group on TWSTFT launched a pilot study in February 2016 for validating the SDR receiver in view of its implementation for use in UTC time links. Participants to this pilot study were the laboratories contributing to UTC which operate the SDR receiver and the BIPM time department. Goals of the pilot study were first, to validate the efficacy of the SDR receiver for improving the TWSTFT uncertainty and significantly reduce the diurnal effects; second to implement routine TW code measurement data through SDR receiver to improve the UTC time comparisons. In the framework of the pilot study, SDR receivers have been installed and are operational since the end of 2016 at TL, NICT, KRIS, NTSC in Asia, PTB, OP and SU in Europe and NIST in the US. The project to install the SDR receiver in all the TW laboratories is ongoing. The analysis of the data obtained from the pilot study shows that in some TW links there is significant improvement, while in others very small or no noise reduction is visible. This result needs more investigation, together with other open points such as the calibration etc. At this step, the results of this pilot project are positive. The development of a SDR achieving complete independence from the currently used SATRE

modems remains necessary, since the present software uses the SDR for the reception of the signal, and keeps the SATRE modem for the signal transmission. Other studies concerning TW development can be found here [77, 78].

6. Other time scale—UTCr

Considering the evolving needs of time metrology and the convenience of allowing the contributing laboratories access to a realization of UTC more frequently than through the monthly *Circular T*, the BIPM time department started in 2012 to implement the computation of UTCr [16], a rapid realization of UTC published every week and based on daily data submitted daily. After 18 months of pilot experiment, UTCr has been declared operational and is now an official publication of the BIPM. Since 1988, UTC has been calculated with one-month data batches at five-day intervals. Extrapolation of values over 10 to 45 days based on prediction models is necessary to many applications. UTC, as published today, is not adapted for real and quasi-real time applications and it was recognized that a more rapid realization would be of benefit to a variety of applications (see section 2 the History of UTC). For these reasons, the BIPM provides UTCr, a new realization of UTC available with a shorter delay. The stability of UTCr was expected to be about comparable to that of UTC, albeit slightly worse because the number of participating clocks would necessarily be smaller and because, in general, a deferred solution (here UTC) is expected to be better than a rapid solution (UTCr). In order to achieve a similar performance, it was decided to use the same algorithm (frequency prediction, weighting scheme) and to apply it in a similar manner with a calculation interval covering approximately one month. UTCr was designed to be a realization of UTC, i.e. in practice the goal is to minimize the time difference [UTCr–UTC]. For this purpose a steering algorithm has to be implemented. In November 2018, 62 laboratories representing 74% of the clock weight in UTC participate to UTCr calculation. The results are published every Wednesday before 18:00 UTC on the web page [54].

6.1. Input data and algorithm

The elaboration of UTCr can be split into four steps:

1. **Data reporting and checking.** Due to the short delay in publication, procedures have been developed to allow the automatic treatment of data and calculation of the solution. In operational use, interaction with laboratories for data checking is significantly reduced. The automatic processing is based on the name of the files and the structure of the ftp directories. Standard file naming conventions must be respected, see [54] for guidelines. Manual handling is required only to allow the inclusion of new data in the data set. With this exception, a number of tasks are automatically carried out in the following steps: continuous detection of incoming files, automatic report of unknown file names, automatic checking of the data format for the known file names, automatic report on

recognized data files and automatic data reminders sent to laboratories on Tuesday 12:00 UTC.

2. **Computation of the time links.** For obtaining results for UTCr close to those of UTC the same time links techniques are used. If the UTC link is GPS P3, GPS MC the UTCr link is the same as the UTC link. If the UTC link is GPSPPP, the corresponding GPS P3 link is used for UTCr. This should cause at most a small additional noise because the statistical uncertainty is estimated at 0.7 ns for a GPS P3 versus 0.3 ns for a GPSPPP link. However no systematic difference is expected because the PPP results use the P3 code as a reference. If the UTC link is TWSTFT or TWGPPP, then either the TWSTFT or the corresponding GPS P3 link is used for UTCr. In the latter case, when large systematic differences exist between the two types, corrections are applied to maintain the differences between UTC and UTCr links below the declared u_{cal} uncertainty reported in section 5 of *Circular T*.
3. **Stability algorithm.** The stability algorithm is similar to the algorithm used for UTC calculation and presented in the previous sections. It consists of two parts: the clock frequency prediction algorithm, and the clock weighting algorithm. The computation interval $[T, T + \tau]$ has a duration between 27 and 31 d, as it starts with a UTC standard date (i.e. a MJD ending with 4 or 9) and ends with the last day of the week under computation. The ensemble scale UTCr is:

$$UTC_r - h_j(t) = \sum_{i=1}^N w_i [h'_i(t) - x_{(i,j)}(t)] \quad (22)$$

where N is the number of participating clocks, w_i the relative weight of clock H_i , $h_j(t)$ is the reading of clock H_j at time t , $x_{i,j} = h_j - h_i$, and $h'_i(t)$ is the prediction of the reading of clock H_i that serves to guarantee the continuity of the timescale as in UTC. In the UTCr algorithm the frequency drift of a clock is taken to be the drift value obtained for that clock in the most recently available monthly UTC computation. The weighting algorithm in UTCr is harmonized to the UTC weighting algorithm. It is complicated to fully implement the same weighting algorithm in UTCr as in UTC. However it is simple to implement a fix that uses the clock variances obtained from the most recent UTC computation to compute UTCr weights similar to UTC. The maximum weight of a clock is set at $2.5/N$; where N is the number of clocks with a non-null *a priori* weight; a test for ‘abnormal behaviour’ is implemented, by checking the difference between the predicted and the real frequency of the clocks.

4. **Steering algorithm.** The steering of UTCr to UTC is done by replacing the past values of [UTCr-Clock] by the values [UTC-Clock] when they become available after each monthly UTC computation. This ensures that the past values of the clock data, used to compute the predictions $h'_i(t)$ in equation (22), never diverge between UTCr and UTC.

6.2. Validation of UTCr and comparison to UTC

To check the quality of UTCr, its difference with UTC has to be evaluated. The direct comparison of UTCr with UTC is a weighted average of the individual differences between UTC and UTCr for each laboratory k , computed at the date t_j as:

$$D(t_j) = \sum_{k=1}^N w_{kj} ([UTCr-UTC(k)](t_j) - [UTC-UTC(k)](t_j)) \quad (23)$$

where w_{kj} is the total weight of the laboratory k in the UTCr calculation at the publication date t_j . Figure 7 shows this direct comparison for six years (August 2012 to December 2018).

Over the interval MJD 56239–58479 (corresponding to August 2012 and December 2018) and UTCr–UTC remains in the interval $[-5.8 \text{ ns} - 7.8 \text{ ns}]$ as can be observed from figure 7, with a mean of 0.02 ns and a RMS of 1.52 ns. Other statistical tools could be applied to check the quality of UTCr as for example by analyzing the 95% of percentile of distribution; using this statistical tool the ‘outliers’ do not affect the results. Several adjustments have been done to the algorithm to maintain the difference between UTC and UTCr as small as possible. Two major actions have been carried out to the UTCr algorithm to improve its stability. The stability algorithm, inclusive of prediction and weighting algorithms, is currently very similar to that of UTC; the effect of wrong data reported for some clocks has been minimized by comparing the clock data submitted for UTCr with those reported for UTC. In their goal to provide an accurate realization of UTC, several time laboratories have devised special algorithms to ensure that their UTC(k) remain close to UTC.

For example, the USNO relies on a set of more than 60 clocks including four Rb fountains [79] that typically make up 25% of the total weight of UTC. In another approach, since February 2010, UTC(PTB) has been realized by steering in frequency an active hydrogen maser to a combination of the primary and commercial caesium clocks of PTB [80]. Such an approach is also pursued at the LNE-SYRTE [81, 82] and in other laboratories. We now compare the performances achieved by the USNO and PTB in the difference [UTC–UTC(k)] with that observed for [UTC–UTCr]: over the interval 56239–58419, [UTC–UTC(USNO)] has a mean of -0.19 ns and a RMS of 1.5 ns and [UTC–UTC(PTB)] has a mean of -0.11 ns and a RMS of 1.47 ns. Therefore the realization of UTC by UTCr is about 50% more accurate than the realizations provided by the major participating laboratories. This result is not unexpected but shows that UTCr fulfills its stated goal. The main statistical data readily available for all weeks of UTCr computation is the number of clocks considered for weighting. The number of clocks represents about 74% of the number of clocks in UTC. The maximum weight w_{max} , which is computed with the same formula as $2.5/N$, is therefore higher in UTCr than in UTC.

In figure 8 the global weight for each laboratory is reported with the corresponding weight in UTC. Looking at the weights gained by the clocks and laboratories, that many of the laboratories that have a significant weight in both UTC and UTCr have a larger relative weight in UTCr (because N is smaller in

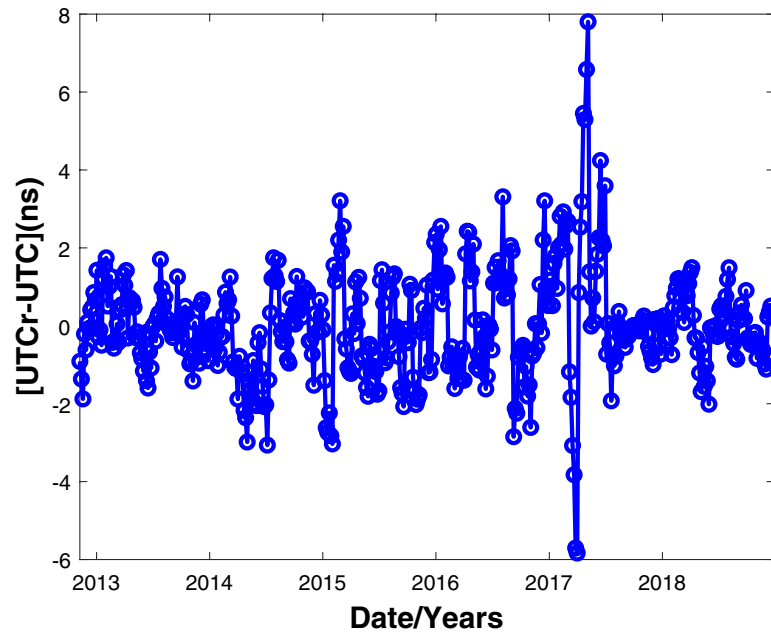


Figure 7. Comparison between UTC and UTCr.

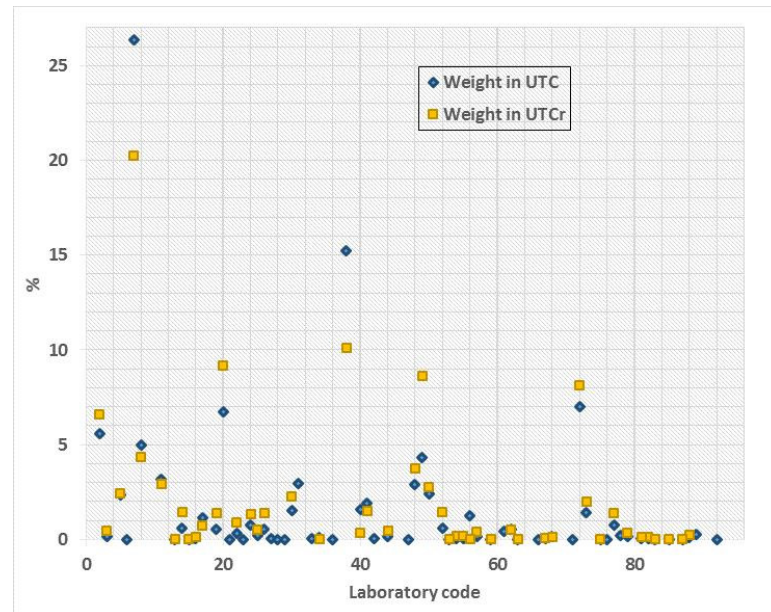


Figure 8. Comparison between the weights in UTC and in UTCr.

UTCr than in UTC). This is expected because each clock has a larger weight due to the reduced number of clocks in UTCr compared to UTC. However, the variability of the weights gained by laboratories is larger in UTCr because, due to the tight schedule of computation, no effort is made to recover late or missing data. On the other hand, due to the overlapping structure of the computation, clocks which happen to miss one week in UTCr fully regain their weight as soon as the missing data are completed.

In figure 9 the number of atomic clocks used in UTC and in UTCr are reported from 2015 to December 2018. The number of clocks eligible for weighting in UTCr has increased until the end of September 2015, and has been maintained, more or less, between 350 and 380 since then (see figure 9).

We can infer that UTCr is about 20% less stable than UTC, considering that it is based on 70% of the clocks with similar characteristics. Following the procedure in [83], we estimate the 1 month instability of UTC to be of order 3.5×10^{-16} over 2015–2017, so that the 1 month instability of UTCr is of order 4×10^{-16} .

Table 2 presents some characteristics related to the weights in UTCr and in UTC over the two months considered above. We see that the one-month instability of clocks at maximum weight is quite constant and similar in UTCr and UTC. It confirms that the structure of the UTCr clock ensemble does not change much and is comparable to that of the UTC ensemble. The main evolution is with the number of participating clocks which then drives the number of clocks at maximum weight

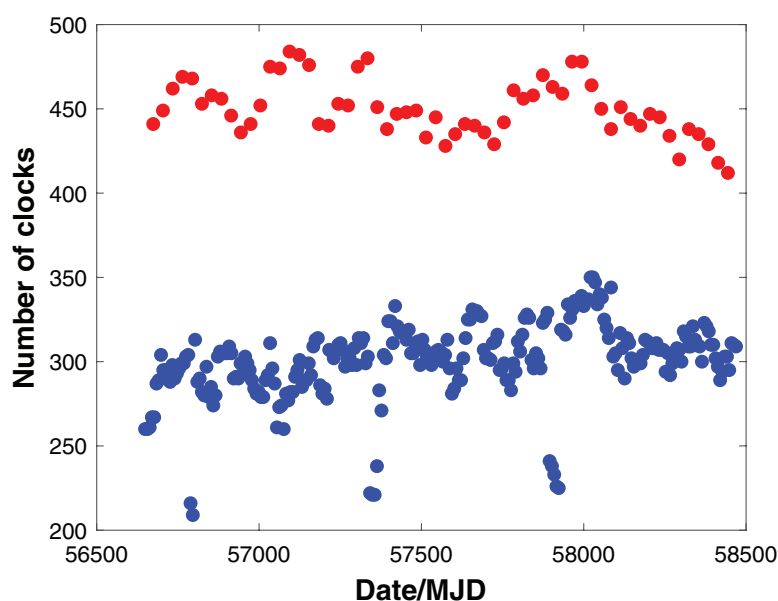


Figure 9. The total number of clocks in UTC (red) and in UTCr (blue).

Table 2. Some characteristics of the clocks forming UTCr and UTC in 2015 and September 2017.

	UTCr 1501	UTC 1501	UTC 1709	UTCr 1743
N clocks with weight	279	452	478	334
Max weight w_{\max}	0.896%	1.036%	0.959%	0.75%
One month instability at w_{\max}	4.1×10^{-15}	4.8×10^{-15}	4.8×10^{-15}	4.1×10^{-15}
Total weight @ w_{\max}	32.3%	70.72%	66.17%	56.9%

and improves correspondingly the stability of the timescale. It is to be noted that there is not a unique method to compute the difference UTCr–UTC. Previously the weighted difference $D(t)$ as defined in equation (23) has been used for evaluating this difference. However each laboratory k will tend to use the difference obtained through its UTC(k) as [UTCr–UTC(k)](t)–[UTC–UTC(k)](t). In the case where the same link is used for laboratory k in UTCr and UTC, the two estimates should be close. If the links are different, the two estimates may be somewhat different and users should be aware of this fact when using [UTCr–UTC(k)] as a prediction of [UTC–UTC(k)]. Obviously there is no means to ensure that the link used for a given UTCr computation is the same as that used for the whole month of the next UTC computation. For most laboratories, UTCr can directly provide a realization of UTC because the average value of [UTCr–UTC(k)]–[UTC–UTC(k)], which would represent an apparent bias between UTCr and UTC, is smaller than typical instabilities due to other sources. For example, over the interval of MJD 56467–58419, [UTCr–UTC(k)]–[UTC–UTC(k)] has an average of -0.05 ns and a standard deviation of 1.5 ns for OP as can be seen in figure 10. In other cases, the statistics may be different but the conclusion remains valid for the vast majority of laboratories participating to UTCr.

7. Other time scale—terrestrial time (TT)

TT is a coordinate time in the geocentric reference system defined by Resolutions of the IAU [84]. TAI provides one

realization of TT but, because has operational constraints, it does not provide an optimal realization. The BIPM therefore computes in deferred time another realization TT(BIPMXX) (XX indicates the year of calculation, for example TT(BIPM18) for 2018) [83], which is based on a weighted average of the evaluations of TAI frequency by the PSFS. The present procedure for computing TT(BIPMXX) is described in [28] and a yearly computation is performed each January, the latest available being TT(BIPM18) available at <ftp://ftp2.bipm.org/pub/tai/ttbipm/TTBIPM.18>. The algorithm used to evaluate TT(BIPMXX) is the same used to evaluate the frequency of EAL (see section 5.1.3), TT(BIPMXX) is a time scale optimized for frequency accuracy.

The basic features of the procedure for computing TT(BIPMXX) are the following:

- The computation starts in 1993 and uses all PFS/SFS measurements submitted to the BIPM since 1992.
- The frequency of EAL with respect to the PFS/SFS is estimated for each month since 1993 following the algorithm in [27], using an estimation for the stability model of EAL which depends on the period considered and improves with time.
- The series of monthly values $f(\text{EAL-TT})$ is smoothed, interpolated and integrated with a 5 day step since MJD 48984 (28 Dec 1992), at which epoch continuity is ensured with previous realizations.

The uncertainty of the monthly estimations of the frequency of EAL with respect to the PFS/SFS, shown in figure 11,

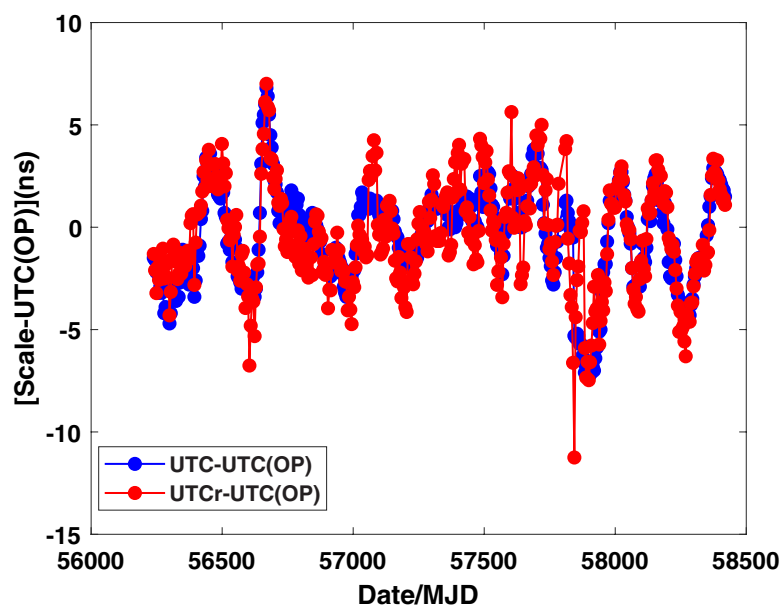


Figure 10. Comparison between UTC–UTC(OP) and UTCr–UTC(OP).

also provides the estimated accuracy of TT(BIPM18). The figure shows that, since 2007, the uncertainty is at or below 5×10^{-16} on average. This is due to the ever increasing number of PSF and SFS evaluations (about 270 since 1999, 81 in 2018 provided by 6 different fountains in 5 different laboratories), and to the improved accuracy of each fountain evaluation. More details on the PFS/SFS evaluations reported to the BIPM may be found in table 6 of the BIPM annual report on time activities [85].

7.1. Evaluation of timescales and of primary frequency standards

TT(BIPMXX) may be considered as the best time reference to be used to compute the instability of TAI and EAL [83], as can be observed in figure 12 where the frequency of TAI with respect PFS/SFS is reported. Here we estimate their instability over the 8 year period 2011–2018 (figure 13), a period over which the performance of the ensemble timescale EAL is more or less constant. For the short term (1 month) TT(BIPM18) is correlated to EAL and TAI so the corresponding values in figure 13 are not significant. For the long term (one year averaging and above), one can see that the behaviour of EAL is red noise and roughly corresponds to a drift. The long-term instability of TAI is between 1×10^{-15} and 2×10^{-15} , a factor two or three worse than the value for TT(BIPM18). TT(BIPM) may also be used to estimate the quality of the PFS/SFS evaluations that contribute to it: first, as TT(BIPM) can be considered a weighted average of the PFS/SFS measurements, the distribution of the values of the frequency differences $f(\text{PFS/SFS}) - f(\text{TT(BIPM18)})$ should fulfill statistical tests, for example we check that the reduced χ^2 is close to 1, see [86] for a detailed study using TT(BIPM05). This confirms that the stated uncertainties of the PFS/SFS evaluations are, in general, statistically sound. This conclusion is supported by the findings of another approach [87] in

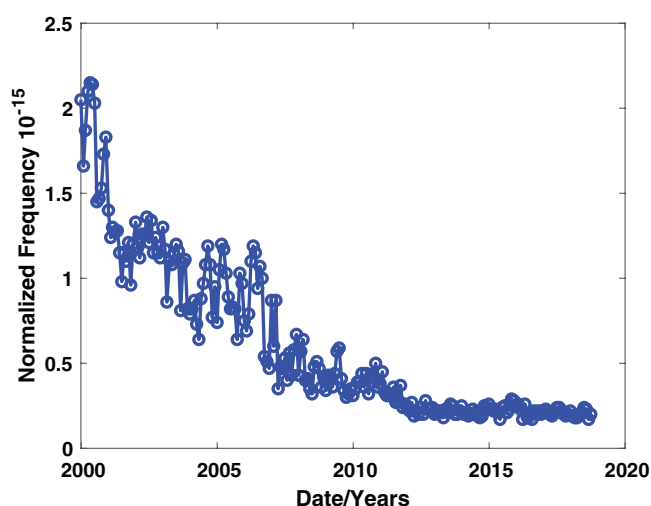


Figure 11. Standard uncertainty of the frequency difference between EAL and TT(BIPM18).

which the evaluations of two or more PFS/SFS are compared when they are close enough in time to be directly linked. These studies bring confidence in the stated uncertainties of the PFS and SFS evaluations, which in turn directly yield the uncertainty estimates of TT(BIPM).

8. Traceability

CCTF criteria for obtaining traceability in time and frequency are published in Guideline 9 of the CCTF WGMRA [88] referring to the document CIPM 2009-24 (13 October 2009) on ‘Traceability in the CIPM MRA’ [89]. The NMIs and DIs contribute to the computation of coordinated universal time (UTC); they maintain local realizations designated by UTC(k), which are traceable to UTC via the key comparison CCTF-K001.UTC, the unique key comparison that has been

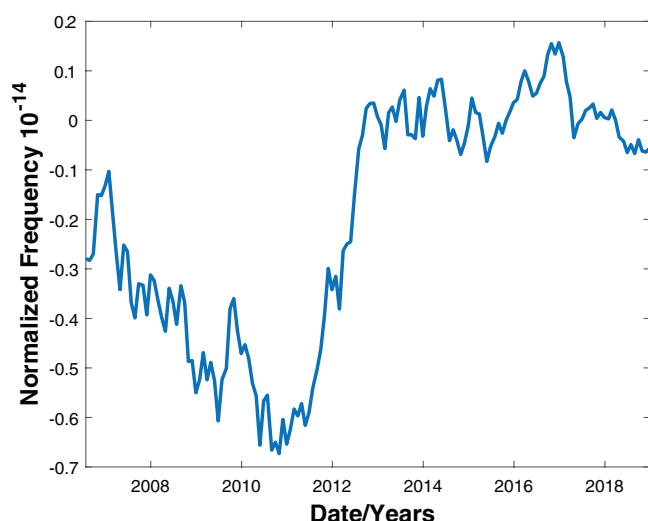


Figure 12. Comparison of the frequency of TAI with respect to PFS/SFS.

defined by the CCTF. NMIs and DIs have two ways of establishing their traceability route to the SI second:

- By participating to the monthly key comparison CCTF-K001.UTC piloted by the BIPM and published in the BIPM KCDB;
- Via another NMI or DI which participates to the key comparison CCTF-K001.UTC having relevant CMCs with appropriate uncertainty published in the BIPM KCDB. In this case, the involved time/frequency comparisons must be first submitted to a process of validation at least at regional level, with a communication to the CCTF WG on MRA for commenting. A fully documented report is to be presented to support the results of the claiming of traceability for the comparison, which shall include the comparison procedure and uncertainty budget.

No alternative paths have been recommended by the CCTF.

9. Dissemination—*Circular T*

The timescales TAI and UTC are disseminated every month through BIPM *Circular T*. Access to UTC is provided in the form of differences [UTC–UTC(*k*)], thus at the same time making the local approximations UTC(*k*) traceable to UTC. As from January 2005, the uncertainties of the differences have also been published [33, 34]. The values of the frequency corrections to TAI, and their intervals of validity, are regularly reported. This information is needed for the laboratories to steer the frequency of their UTC(*k*) to UTC. *Circular T* provides wide access to the best realization of the second through the estimation of the fractional deviation *d* of the scale interval of TAI with respect to its theoretical value based on the SI second, calculated as explained in section 5. The values of *d* for the individual contributions of the PFS and SFS are also published, giving access to the second as realized by each standard.

With the aim of supporting users of GNSS systems, information on the offsets between UTC and TAI and the predictions of UTC(USNO) and UTC(SU) broadcast by GPS and

GLONASS has been provided since January 2011 in *Circular T*. Also access to GPS time with an uncertainty of a few nanoseconds and to GLONASS time with an uncertainty of a few tens of nanoseconds is provided via their differences with respect to TAI and UTC in the time department ftp server [54]. This information should not be considered as a source of traceability to UTC of the respective UTC(*k*) predictions broadcast by the GNSS and of the GNSS times, since they do not fulfill the metrological criteria for obtaining traceability described in section 8.

Each monthly issue of *Circular T* from January 2016 provides information on the time links used for that particular computation, including the technique and equipment used for the comparisons and the respective uncertainties, split into three components: the uncertainty characterizing the link instability (noise), the uncertainty of the equipment calibration at the moment of the calibration measures, and the uncertainty added due to the aging of the calibration. In case that new (uncalibrated) equipment is introduced, an additional 1 ns uncertainty is included coming from the alignment procedure to the former link. The ftp server of the BIPM time department [54] gives access to clock data and time transfer files provided by the participating laboratories, as well as the rates and weights for clocks in TAI in each month of calculation. This information is particularly useful for laboratories in the study of their clocks behaviour. Results for a complete year are published in the BIPM annual report on time activities [85], together with information about the equipment in contributing laboratories, time signals and time dissemination services, as reported by the laboratories to the BIPM. *Circular T* is published in html version with linkable information such as data used, plots, available reports and documents. Additional information is published on the time department ftp server [54]. The information about time link calibration has been formalized by assigning to each calibration an identifier corresponding to a calibration report. The calibration report is under the responsibility of the coordinating laboratory, as for example the BIPM for the regional nodes identified as G1 group laboratories (details can be found in section 5.4), or a G1 laboratory responsible for a calibration within its metrology region.

Since 2016 dynamic information on participants, equipment, calibrations, and interactive plots is provided via the data base at [90].

10. Future improvements

In this section we discuss the possible developments of UTC [20]. Different aspects are considered, including the role of fountains in the formation of the time-scale, the possibility of achieving a fountain-only time-scale, the impact of newly developed clocks, time link redundancy and rapid time-scale solutions.

10.1. Long-term stability and the impact of new frequency standards

The number of atomic fountains reporting data to the BIPM has continuously increased over the past decade. Since 2012, data

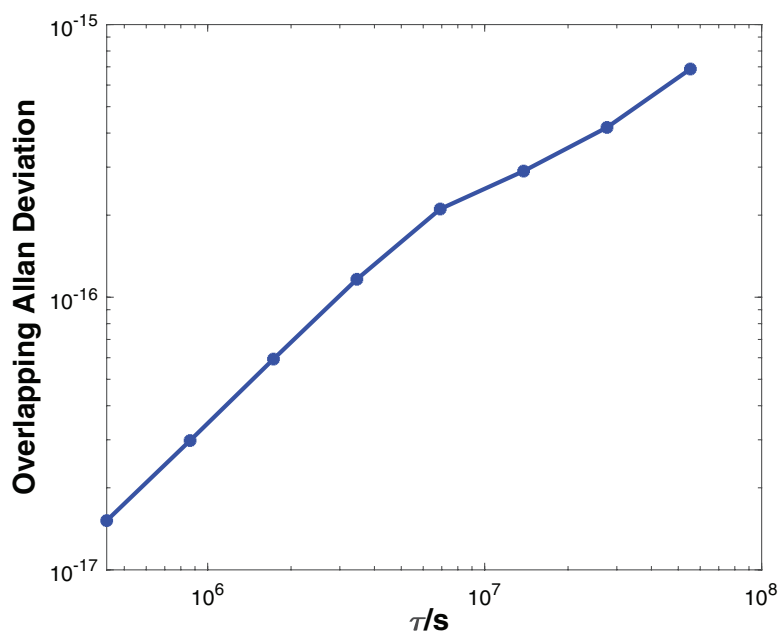


Figure 13. Stability analysis of $y(\text{EAL})-y(\text{TT})$.

from atomic fountains, either clocks or frequency standards, are numerous enough to allow their sole use in the formulation of a timescale. This is principally due to the presence of four USNO Rb fountains continuously operated as clocks [91], but existing primary and secondary standards are also marginally sufficient to form a timescale by themselves. As an example, test timescales have been computed over 630 d in 2012–2013 using data from (up to) 10 fountains [92, 20]. It is shown that such fountain-only timescales have a long-term (40–80 days) instability which is of the order of 2×10^{-16} , comparable to that of the realization of terrestrial time, computed yearly at the BIPM, TT(BIPM). Such fountain-only time scales are nearly independent of EAL/TAI for averaging durations up to a few months. On one hand, some fountains operated as clocks do contribute to EAL but their weight is limited to the maximum weight in the algorithm used for UTC calculation, of the order of 1% each. On the other hand, fountains operated as primary standards do have correlations with EAL/TAI through the frequency steering and the frequency prediction algorithm but this correlation is for an averaging duration of several months. Indeed, in the quadratic frequency prediction the BIPM implemented for clocks in EAL, the frequency drift is estimated with respect to TT(BIPM) over a three-month interval [22, 24]. Also the steering procedure has a characteristic time constant of several months because it is announced two months in advance and takes into account several months of past observations; with the implementation of the new computation algorithm (refer to section 5.1) almost no monthly steering has been necessary for TAI since September 2012, only additional corrections were necessary between October 2016 and September 2017. For these reasons, fountain-only timescales are nearly independent of EAL/TAI and are a useful tool to estimate its instability up to an averaging duration of a few months.

Such fountain-only scales are still not robust enough because of the small number of devices and of laboratories

involved, but they are promising and may be a way forward for the future generation of TAI and UTC. In addition other clock designs may provide the same kind of long-term instability and continuous operation needed to generate the reference timescale. For example efforts are underway at NASA/JPL to develop a frequency standard based on the hyperfine transition at 40.5 GHz in $^{199}\text{Hg}^+$ ions [93] or 29.95 GHz in $^{201}\text{Hg}^+$ ions [94] trapped in a linear ion trap. For the $^{199}\text{Hg}^+$ transition, a instability floor of less than 2×10^{-16} and a drift lower than $2.7 \times 10^{-17} \text{ d}^{-1}$ have been reported.

Assuming a few tens of such clocks are independently operated in a number of laboratories world-wide, they could be used to generate a robust timescale with instability at 1×10^{-16} and below for averaging durations between 10 d to months. This would fulfill all present needs for the time instability of a reference time scale: for example a one-month time instability in the hundreds of ps would be of the order of the noise of the present best time transfer techniques generally used to access it; also a one-year time instability in the 1–2 ns would be lower than the most optimistic measurement noise of pulsar timing, for example using the future square kilometer array telescope [95]. If these clocks become available, the main obstacle to obtain the full performance of such a timescale may be limitations in time transfer techniques (see section below).

10.2. Towards real time time-scale realizations, predictions and redundant time transfer measurements

Considering the evolving needs and the new developments of time metrology, we will be faced with reviewing the strategy for the generation of UTC in the near future. The algorithms developed to calculate UTC should reflect the new scientific discoveries and new physical realities and the accessibility of UTC should follow the requests of time laboratories and users.

The network of time links used in the generation of UTC until now is supported by two independent techniques; two-way satellite time and frequency transfer and uni-directional comparisons based on GNSS observations. Several types of measurements exist for GNSS time transfer, for example single frequency code, dual frequency code, dual frequency code and phase for GPS. Moreover new satellite systems such as the global Galileo (Europe) and BeiDou (China), and the regional QZSS (Japan) and IRNSS (India) will provide, in the near future, an increasing number of measurements. For the TWSTFT in Europe, North America and Asia, a complete set of redundant measurements is available; new modems are being developed and some more are expected to come onto the market. A better, global use of this ensemble of measurements will optimize the impact of the time links in UTC calculation by improving its metrological properties.

A possible way to make full use of these systems and to better exploit all the available measurements is to use redundant time links to solve the time scale system [55]. Following this approach, the system of the time links is solved by the least square method weighted with respect to the corresponding uncertainty.

As presented in section 6 in 2012 the BIPM time department implemented the computation of a rapid UTC solution (UTC_r) to provide the convenience of allowing the contributing laboratories access a realization of UTC more frequently than through the monthly *Circular T*, and consequently to assess on a shorter delay the level of synchronization of the local UTC(k) to the international reference. A next development could therefore be a real time prediction of UTC. In such a way all users could have a real time access to UTC, with particular impact on the synchronization of GNSS system times to the international reference.

10.3. Possible limitations of time transfer techniques

The time transfer techniques presently used in the generation of TAI are TWSTFT and techniques using GNSS phase and code measurements. Time links using GNSS phase and code achieve time instability of about 100 ps over one day (i.e. 1×10^{-15} in frequency) to about 300 ps over one month (i.e. 1×10^{-16} in frequency) [44, 96]. The operational performance of TWSTFT is also of the same order of magnitude [96], limited by severe constraints in signal strength, bandwidth and cost of renting the use of geostationary satellites. Some improvement may be expected for GNSS techniques for example through new systems that bring more measurements and new codes such as the Galileo E5 signal [97, 98]; new processing techniques should also improve results with the present measurements, for example through the use of integer ambiguity resolution (IPPP) [68, 99]. For TWSTFT also, some improvement could be brought to the time transfer results by buying more bandwidth and more satellite transponder time; in addition new techniques are being developed, such as using bandwidth-synthesis [77] or using the carrier phase [78]. Although the latter technique could bring order of magnitude improvement, it is unlikely to be practical to operate

with commercial geostationary satellites. Present techniques are therefore likely to be limited around the 1×10^{-16} level, at averaging times of no less than several days.

Obviously phase + code two-way microwave operation would be a way to go but will need a dedicated space payload to overcome the operational constraints of using geostationary communication satellites. The prototype in this category is the ACES microwave link [70, 71] due to fly with the ACES mission in 2020. Its expected time instability is about 7 ps at one-day (1×10^{-16}) and about 20 ps at ten-day averaging (2×10^{-17}). Free space optical techniques may also be promising. The most advanced satellite time transfer system currently in operation is T2L2 (time transfer by laser light) onboard the Jason 2 satellite [100]. However such techniques, which depend on the weather will always be limited for operational Earth-based time transfer.

For several years, a number of developments have occurred that use optical fibres for frequency comparisons and, more recently for disseminating time signals using a single fibre to avoid uncorrelated noise over two fibres. Among those, one technique using active stabilization and calibration of the propagation delay [101, 102] was demonstrated on optical paths of several hundred kilometers with an accuracy of the order of a few tens of ps and a time deviation below 1 ps up to one-day averaging (for example a frequency instability of order 10^{-17}). Another technique uses the usual two-way method and equipment to their full bandwidth capability and was demonstrated on a distance of 70 km with an accuracy below 100 ps [103], and on a 540 km fibre link also used for frequency transfer with an accuracy of order 250 ps and a time instability (1 d) of order 20 ps [104]. In all cases, it seems that systematic effects (delay calibration, power sensitivity, fibre chromatic dispersion, polarisation mode dispersion) can be characterized to less than 50 ps, therefore these techniques provide the best time transfer accuracy and can be used as a reference to calibrate other techniques. One can therefore envision that these techniques will be fundamental for frequency transfer over continental regions and they could also provide time transfer with unprecedented calibration accuracy. Such fibre networks are currently being implemented, in particular in Europe, see for example the Joint Research Project NEAT-FP of the European Metrology Research Programme aiming at accurate time/frequency comparison and dissemination through optical telecommunication networks [105]. However, as such optical fibre links require amplifier stations about every 100 km, they are not suited to intercontinental links.

In an ideal case, we could have an ‘ACES-like’ technique providing accurate time links between selected ‘hubs’ between different continents and networks of optical fibres providing accurate time links within the continents, therefore providing world-wide time transfer at a level of 10–100 ps for all averaging times. This could revive (with 2 orders of magnitude improvement) the situation in around year 2000 when the UTC network was based on a few intercontinental links with all other shorter-distance links within continents. Such a situation is unlikely to happen in the near future because no ‘ACES-like’ technique is expected to be available for

long-term operation after the ACES mission, and also because the realization of the continental networks of optical fibres for time transfer will take time, but it could be a medium-term goal. In the shorter term, a more realistic situation is with one technique (GNSS phase and code) providing time links with a similar level of performance for all UTC stations, with one much more accurate technique (optical fibre) available on selected links and possibly other techniques (for example TWSTFT) available on some other links with various levels of performance. This is a case where it is desirable to use all available information, solving a redundant system of time links to provide the most accurate solution for TAI (see previous section).

Acknowledgment

The authors would like to thank the BIPM Department staff for helpful discussions; to Aurélie Harmegnies, Federica Parisi, Gérard Petit and Laurent Tisserand for having agreed on the use of materials already published in common papers, and the time laboratories for their participation to the computation of UTC.

References

- [1] Terrien J 1971 News from the Bureau International des Poids et Mesures *Metrologia* **7** 43–4
- [2] BIPM 1969 *Comptes Rendus de la 13e CGPM (1967/68)* 103
- [3] Terrien J 1968 News from the Bureau International des Poids et Mesures *Metrologia* **4** 43
- [4] ITU 2008 ITU-R Recommendations Reports, TF series and recommendation ITU-R TF.460-6
- [5] Essen L and Parry J 1955 Atomic standard of frequency and time interval *Nature* **176** 280–2
- [6] BIPM 1997 CIPM Report of the 86th Meeting (September 1997), Tome 65 (available from www.bipm.org)
- [7] IAU, all IAU resolutions may be found at www.iau.org/administration/resolutions/generalassemblies/
- [8] ITU 1970 CCIR XIIth Plenary Assembly 183
- [9] BIPM 1972 14th General Conf. on Weights, Measures and Comptes Rendus de la 14e CGPM 1971 p 77
- [10] Terrien J 1972 News from the Bureau International des Poids et Mesures *Metrologia* **8** 35
- [11] BIPM 2019 26th CGPM resolution B (available from www.bipm.org)
- [12] Terrien J 1975 News from the Bureau International des Poids et Mesures *Metrologia* **11** 180
- [13] ITU, all ITU-R recommendations may be found at (www.itu.int/pub/R-REC)
- [14] McCarthy D D 2011 Evolution of time scales from astronomy to physical metrology *Metrologia* **48** S132–44
- [15] BIPM Circular T (available from www.bipm.org)
- [16] Petit G, Arias F, Harmegnies A, Panfilo G and Tisserand L 2014 UTCr: a rapid realization of UTC *Metrologia* **51** 33–9
- [17] BIPM 2019 *Le SYSTEME Int. d'Unités SI* 9th edn
- [18] Panfilo G and Arias E F 2010 Algorithms for TAI *UFFC* **57** 140–50
- [19] Arias E F, Panfilo G and Petit G 2011 Timescales at the BIPM *Metrologia* **48** 145–53
- [20] Petit G, Arias E F and Panfilo G 2015 International atomic time: status and future challenges *C. R. Phys.* **16** 480–8
- [21] Panfilo G and Arias E-F 2010 Studies and possible improvements on EAL algorithm *UFFC* **57** 154–60
- [22] Panfilo G, Harmegnies A and Tisserand L 2012 A new prediction algorithm for the generation of international atomic time *Metrologia* **49** 49–56
- [23] Guinot B and Thomas C 1988 Establishment of international atomic time *Annu. Rep. BIPM Time Sect.* **1** A3–A6 (Available from the BIPM website www.bipm.org)
- [24] Panfilo G, Harmegnies A and Tisserand L 2014 A new weighting procedure for UTC *Metrologia* **51** 285–92
- [25] Panfilo G 2016 The coordinated universal time *Special Issue Women Contrib. IEEE Instrum. Meas. Mag.* **19** 28–33
- [26] Guinot B 1987 Some properties of algorithms for atomic time scales *Metrologia* **24** 195–8
- [27] Azoubib J, Graveaud M and Guinot B 1977 Estimation of the scale unit duration of time scales *Metrologia* **13** 87–93
- [28] Petit G 2003 A new realization of terrestrial time *Proc. 35th Precise Time and Time Interval (PTTI) Meeting* pp 307–16
- [29] Allan D-W and Weiss M-A 1989 The NBS atomic time scale algorithm: AT1, NBS Tech. Note 1316
- [30] Levine J 1999 Introduction to time and frequency metrology *Rev. Sci. Instrum.* **70** 2567–96
- [31] Panfilo G and Tavella P 2008 Atomic clock prediction based on stochastic differential equations *Metrologia* **45** S108–16
- [32] Petit G 2003 Towards an optimal weighting scheme for TAI computation *Metrologia* **40** S252–6
- [33] Lewandowski W, Matsakis D, Panfilo G and Tavella P 2006 The evaluation of uncertainties in [UTC–UTC(k)] *Metrologia* **43** 278–86
- [34] Lewandowski W, Matsakis D, Panfilo G and Tavella P 2008 Analysis of correlations, and link and equipment noise in the uncertainties of [UTC–UTC(k)] *IEEE Trans. Ultrason. Ferroelectr. Freq. Control* **55** 750–60
- [35] CCTF/1724: (Working document of CCTF meeting 2017 available from BIPM website www.bipm.org)
- [36] Parisi F and Panfilo G 2016 A new approach to UTC calculation by means of the Kalman filter *Metrologia* **53** 1185–92
- [37] Senior K, Koppang P and Ray J 2003 Developing an IGS timescale *IEEE Trans. Ultrason. Ferroelectr. Freq. Control* **50** 585–93
- [38] Defraigne P, Petit G and Bruyninx C 2001 Use of geodetic receivers for TAI *Proc. 33rd Precise Time and Time Interval (PTTI) Meeting* (Long Beach, CA)
- [39] Allan D W and Weiss M A 1980 Accurate time and frequency transfer during common-view of a GPS satellite *Proc. Frequency Control Symp. (Philadelphia, PA)* pp 334–6
- [40] Fujieda M *et al* 2004 Effects of ionospheric correction on GPS time transfer throughout Asia *Metrologia* **41** 145–51
- [41] Petit G and Jiang Z 2008 GPS all in view time transfer for TAI computation *Metrologia* **45** 35–45
- [42] Defraigne P, Bruyninx C, Clarke J, Ray J and Senior K 2001 Time transfer to TAI using geodetic receivers *Proc. European Frequency and Time Forum (EFTF)* (Neuchâtel, Switzerland) pp 517–21
- [43] Kouba J and H'eroux P 2001 Precise point positioning using IGS orbits and clock products *GPS Solut.* **4** 31
- [44] Petit G and Jiang Z 2008 Precise point positioning for TAI computation *Int. J. Navig. Obs.* **56** 2878
- [45] Allan D W and Thomas C 1994 Technical directives for standardization of GPS time receiver software *Metrologia* **31** 69–79
- [46] Defraigne P and Petit G 2015 CGGTTS-Version 2E: an extended standard for GNSS *Metrologia* **52** G1
- [47] International GNSS Service (IGS) 2015, RINEX Working Group and Radio Technical Commission for Maritime Services Special Committee 104 (RTCM-SC104), The receiver independent format exchange (<ftp://igs.org/pub/data/format/rinex303.pdf>)

- [48] Lewandowski W and Jiang Z 2009 Use of Glonass at the BIPM *Proc. PTTI 2009 (Santa Ana Pueblo, NM)* pp 5–13
- [49] Jiang Z and Lewandowski W 2012 Use of GLONASS for UTC time transfer *Metrologia* **49** 57–61
- [50] Defraigne P, Baire Q and Harmegnies A 2011 Time and frequency transfer combining GLONASS and GPS data *Proc. 42th Precise Time and Time Interval (PTTI) (Reston, VA)* pp 263–74
- [51] Hanson D W 1989 Fundamentals of two-way time transfers by satellite *43rd Annual Symp. on Frequency Control* pp 174–8
- [52] Kirchner D 1991 Two-way time transfer via communication satellites *Proc. IEEE* **19** 983–90
- [53] ITU, International Telecommunication Union TF Series, Recommendation TF.1153-4, The operational use of two-way satellite time and frequency transfer employing pseudorandom noise codes 2015 (available from ITU website www.itu.int)
- [54] BIPM FTP server of the BIPM time department (available from www.bipm.org)
- [55] Petit G and Jiang Z 2006 Using a redundant time links system in TAI computation *Proc. of the 20th EFTF* pp 436–9
- [56] Jiang Z and Petit G 2009 Combination of TWSTFT and GNSS for accurate UTC time transfer *Metrologia* **46** 305–14
- [57] Lewandowski W and Moussay P 2002 Rapports BIPM-2002/02; BIPM-2003/04; BIPM-2003/05 (available from www.bipm.org)
- [58] Lewandowski W and Tisserand L 2004 Rapports BIPM-2004/05 BIPM-2004/06, BIPM-2004/08 (available from www.bipm.org)
- [59] BIPM, BIPM guidelines for GPS equipment calibration (available from www.bipm.org)
- [60] Jiang Z, Arias E F, Lewandowski W and Petit G 2011 BIPM calibration scheme for UTC time links *Proc. IFCS-EFTF* pp 1064–9
- [61] Matsakis D 2003 *Proc. 34th PTTI (Reston, VA)* pp 437–56
- [62] Cordara F *et al* 2004 Calibration of the IEN-PTB TWSTFT link with a portable reference station *Proc. 18th European Frequency and Time Forum (EFTF) (Guildford, UK)* pp 121–3
- [63] Lewandowski W, Cordara F, Lorini L, Pettiti V, Bauch A, Piester D and Koudelka O 2004 A simultaneous calibration of the IEN/PTB time link by GPS and TWSTFT portable equipment *Proc. 18th Proc. European Frequency and Time Forum (EFTF) (Guildford, UK)* pp 1–7
- [64] Piester D, Hlavac R, Achkar J, de Jong G, Blanzano B, Ressler H, Becker J, Merck P and Koudelka O 2006 Calibration of four European TWSTFT Earth stations with a portable station through Intelsat 903 *Proc. 19th European Frequency and Time Forum (EFTF) (Besancon, France)* pp 354–9
- [65] BIPM 2016, TWSTFT calibration guidelines for UTC time links (available from www.bipm.org)
- [66] Achkar J, Fujieda M, Riedel F, Takiguchi H, Beukler E, Piester D 2016 Study of the OP-PTB link by carrier-phase two-way satellite time and frequency transfer, at CPEM 2016 <https://doi.org/10.1109/CPEM.2016.7540721>
- [67] Fujieda M, Gotoh T and Amagai J 2016 Advanced TWSTFT by carrier-phase and carrier-frequency measurements *J. Phys.: Conf. Ser.* **723** 012036
- [68] Petit G, Kanj A, Loyer S, Delporte J, Mercier F and Perosanz F 2015 1×10^{-16} frequency transfer by GPS PPP with integer ambiguity resolution *Metrologia* **52** 301–9
- [69] Fujieda M *et al* 2018 Advanced satellite-based frequency transfer at the 10^{-16} level *IEEE Trans. UFFC* **65** 973–8
- [70] Salomon C, Cacciapuoti L and Dimarcq N 2007 Atomic clock ensemble in space: an update *Int. J. Mod. Phys. D* **16** 2511
- [71] Meynadier F, Delva P, le Poncin-Lafitte C, Guerlin C and Wolf P Atomic clock ensemble in space (ACES) data analysis *Class. Quantum Grav.* **35** 035018
- [72] Guena J *et al* 2017 First international comparison of fountain primary frequency standards via a long distance optical fibre link *Metrologia* **54** 348–54
- [73] Ido T *et al* 2017 Activities of time and frequency metrology at NICT: optical and microwave frequency standards and their remote comparisons *The Science of Time 2016* (New York: Springer)
- [74] Jiang Z *et al* 2018 *Metrologia* **55** 685
- [75] Huang Y J, Tseng W H, Lin S Y, Yang S H and Fujieda M 2016 TWSTFT results by using software-defined receiver data *Proc. European Frequency and Time Forum (York, UK, April 2016)* pp 137–40
- [76] Huang Y J, Fujieda M, Takiguchi H, Tseng W H and Tsao H W 2016 Stability improvement of an operational two-way satellite time and frequency transfer system *Metrologia* **53** 881–90
- [77] Amagai J and Gotoh T 2010 Development of two-way time and frequency transfer system with dual pseudo random noises *J. Natl Inst. Inf. Commun. Technol.* **57** 197–207
- [78] Fujieda M *et al* 2014 Carrier-phase two-way satellite frequency transfer over a very long baseline *Metrologia* **51** 253–62
- [79] Matsakis D N 2012 Time and Frequency Activities at the U.S. Naval Observatory *Proc. 44th Precise Time and Time Interval (PTTI) Reston (Virginia USA)* pp 11–28
- [80] Bauch A, Weyers S, Piester D, Staliuniene E and Yang W 2012 Generation of UTC(PTB) as a fountain-clock based time scale *Metrologia* **49** 180
- [81] Rovera D, Abgrall M, Bize S, Chupin B, Guena J, Laurent P, Rosenbusch P and Urich P 2013 The new UTC(OP) based on the LNE-SYRTE atomic fountains *Proc. Joint IEEE Int. Frequency Control Symp. (IFCS) and European Frequency and Time Forum (EFTF) Prague (Czech Republic)*
- [82] Rovera G D *et al* 2016 UTC(OP) based on LNE-SYRTE atomic fountain primary frequency standards *Metrologia* **53** S81
- [83] Petit G 2007 The long-term stability and accuracy of EAL and TAI (revisited) *Proc. 21st EFTF (Geneva, Switzerland)* pp 391–4
- [84] Guinot B 1988 *Astron. Astrophys.* **192** 370–3
- [85] BIPM Time Department Annual Report (available from www.bipm.org)
- [86] Wolf P *et al* 2006 Comparing high accuracy frequency standards via TAI *Proc. 20th EFTF (Braunschweig, Germany)* pp 476–85
- [87] Parker T 2010 Long term comparison of caesium fountain primary frequency standards *Metrologia* **47** 1–10
- [88] CCTF WGMRA Guideline 9 CCTF criteria for obtaining traceability in time and frequency (available from www.bipm.org)
- [89] CIPM 2009 Traceability in the CIPM MRA (available from www.bipm.org)
- [90] Konaté H and Arias E F 2014 The BIPM time department database *Proc. 45th PTTI Meeting* pp 1–13
- [91] Peil S *et al* 2014 Evaluation of long term performance of continuously running atomic fountains *Metrologia* **51** 263–9
- [92] Petit G 2013 A timescale based on the world's fountain clocks *Proc. 45th PTTI Meeting* pp 265–8
- [93] Burt E A, Diener W A and Tjoelker R L 2008 A compensated multi-pole linear ion trap mercury frequency standard for ultra-stable timekeeping *IEEE Trans. UFFC* **55** 2586–95
- [94] Burt E A, Taghavi-Larigani S and Tjoelker R 2010 A new trapped ion atomic clock based on 201Hg^+ *IEEE Trans. UFFC* **57** 629–35

- [95] Cordes J M *et al* 2004 *New Astron. Rev.* **48** 1413
- [96] Bauch A *et al* 2006 Comparison between frequency standards in Europe and the US at the 10^{-15} uncertainty level *Metrologia* **43** 109–20
- [97] Defraigne P *et al* 2013 Advances in multi-GNSS time transfer *Proc. Joint European Frequency and Time Forum and International Frequency Control Symp. EFTF/IFC* pp 508–12
- [98] Martínez-Belda M C, Defraigne P and Bruyninx C 2013 On the potential of Galileo E5 for time transfer *IEEE Trans. UFFC* **60** 121–31
- [99] Delporte J *et al* 2008 GPS carrier phase time transfer using single difference integer ambiguity resolution *Int. J. Navig. Obs.* **27** 3785
- [100] Exertier P *et al* 2010 Status of the T2L2/Jason2 experiment *Adv. Space Res.* **46** 1559–65
- [101] Krehlik P *et al* 2012 *IEEE Trans. Instrum. Meas.* **61** 2573–80
- [102] Sliwczynski L *et al* 2013 *Metrologia* **50** 133–45
- [103] Rost M, Piester D, Yang W, Feldmann T, WŁubben T and Bauch A 2012 Time transfer through optical fibres over a distance of 73 km with an uncertainty below 100 ps *Metrologia* **49** 772–8
- [104] Lopez O *et al* 2013 Simultaneous remote transfer of accurate timing and optical frequency over a public fibre network *Appl. Phys. B* **110** 3–6
- [105] www.ptb.de/emrp/neatfthome.html